ORDNANCE RESEARCH LABORATORY

THE PENNSYLVANIA STATE UNIVERSITY
UNIVERSITY PARK, PENNSYLVANIA

General Instability of Circumferentially Stiffened Sandwich Shells Subjected to Uniform External Pressure

SERIAL NO. NOrd 16597-91

December 10, 1962

Copy No. 24

NAVY DEPARTMENT • BUREAU OF NAVAL WEAPONS • CONTRACT NORD 16597

General Instability of Circumferentially Stiffened Sandwich Shells Subjected to Uniform External Pressure

By J. D. Stachiw

ORDNANCE RESEARCH LABORATORY

The Pennsylvania State University

University Park, Pennsylvania

December 10, 1962

APPROVED FOR DISTRIBUTION

Leonard J. Kegl, Jr.

ASSISTANT DIRECTOR

APPROVED FOR DISTRIBUTION

John C. Johnson

DIRECTOR

SERIAL NO. NOrd 16597-91

Distribution List

Chief, Bureau of Naval Weapons (RU-2) Department of the Navy Washington 25, D. C.	1 copy
Chief, Bureau of Naval Weapons (RUTO-33) Department of the Navy Washington 25, D. C.	2 copies
Chief, Bureau of Naval Weapons (RUDC) Department of the Navy Washington 25, D. C.	1 copy
Chief, Bureau of Naval Weapons (RUSD) Department of the Navy Washington 25, D. C.	1 copy
Chief, Bureau of Naval Weapons (DLI-3) Department of the Navy Washington 25, D. C.	2 copies
Chief, Naval Operations (OP 721) Department of the Navy Washington 25, D. C. For: IEP AEC 28	5 copies
Chief, Naval Operations (OP 31) Department of the Navy Washington 25, D. C.	1 copy
Chief, Naval Operations (OP 312) Department of the Navy Washington 25, D. C.	1 copy
Chief, Naval Operations (OP 71) Department of the Navy Washington 25, D. C.	1 copy
Chief, Naval Operations (O3EG) Department of the Navy Washington 25, D. C.	1 copy
Chief, Naval Operations (OP07TC) Technical Analysis and Advisory Group Rm5E613, Pentagon Washington 25, D. C.	1 copy
Chief, Bureau of Ships Department of the Navy Washington 25, D. C.	3 copies
Commander Armed Services Technical Information Agency Attention TIPDR Arlington Hall Station Arlington 12, Virginia	10 copies
Commanding Officer U. S. Naval Underwater Ordnance Station Newport, Rhode Island	2 copies
Commander U. S. Naval Ordnance Laboratory White Oak Silver Spring 19, Maryland	2 copies
Commander U. S. Naval Ordnance Laboratory White Oak Silver Spring 19, Maryland Attn: Dr. S. J. Raff	1 copy
Commander U. S. Naval Ordnance Test Station 3202 East Foothill Boulevard Pasadena Annex Pasadena 8, California	2 copies
Commanding Officer U. S. Naval Torpedo Station Keyport, Washington	1 copy
Commanding Officer U. S. Naval Torpedo Station Quality Evaluation Technical Library Keyport, Washington	1 copy
Officer in Charge U. S. Navy Central Torpedo Office Newport, Rhode Island	1 copy
Director (Code 2021) U. S. Naval Research Laboratory Washington 25, D. C.	3 copies
Director (Code 2027) U. S. Naval Research Laboratory Washington 25, D. C.	1 copy
Commanding Officer and Director U. S. Navy Electronics Laboratory San Diego 52, California	1 copy
Commanding Officer and Director David Taylor Model Basin Washington 7, D. C.	1 copy
Commanding Officer U. S. Navy Mine Defense Laboratory Panama City, Florida	1 copy
Commanding Officer and Director U. S. Navy Underwater Sound Laboratory Fort Trumbull New London, Connecticut	1 copy
Commander U. S. Naval Missile Center Point Mugu Port Hueneme, California	1 copy

Commander U. S. Naval Air Development Center Johnsville, Pennsylvania	1 copy
Officer in Charge Naval Aircraft Torpedo Unit Naval Air Station Quonset Point, Rhode Island	1 copy
Scientific and Technical Information Facility P. O. Box 5700 Bethesda, Maryland Attn: NASA Representative (S-AK/DL)	1 copy
Director, Applied Physics Laboratory University of Washington Seattle, Washington	2 copies
Director, Marine Physical Laboratory Scripps Institution of Oceanography San Diego 52, California	1 copy
Hudson Laboratories Dobbs Ferry, New York	1 copy
Commander, Test and Evaluation Force U. S. Atlantic Fleet U. S. Naval Base Norfolk 11, Virginia	1 copy
Clevite Ordnance 540 East 105th Street Cleveland, Ohio	1 copy
Vitro Corporation of America 14,000 Georgia Avenue Silver Spring, Maryland	1 copy
Westinghouse Electric Corporation Lansdowne Plant Baltimore, Maryland	1 copy
Woods Hole Oceanographic Institution Woods Hole, Massachusetts	1 copy
Aerojet General Corporation Azusa, California Attn: G. M. McRoberts	1 copy

Abstract

THE Bresse equation for the buckling of rings under radial pressure is modified to predict the general-instability collapse pressure of cellular sandwich shells under hydrostatic pressure. The validity of the equation is demonstrated by implosion experiments with carefully designed cellular sandwich shells, the general-instability collapse pressures of which are compared with the results obtained by the modified Bresse equation. The results indicate that the modified equation predicts the general-instability collapse pressure of cellular sandwich shells within 5 per cent. This equation is recommended for use only when the ratio of shell ring depth to shell mean diameter is less than 0.1.

Acknowledgment

THIS REPORT is based on research required for the degree of Master of Science at the College of Engineering and Architecture, The Pennsylvania State University. This research, which is described in the thesis "General Instability of Circumferentially Stiffened Sandwich Shells Subjected to Uniform External Pressure," was performed at the Ordnance Research Laboratory from 1959 to 1961. The author wishes to acknowledge the financial and administrative assistance extended by the Ordnance Research Laboratory and the guidance in the writing of the thesis provided by the Mechanics Department of the College of Engineering and Architecture.

Table of Contents

List of Illustrations*

*Illustrations will be found at the end of the report, following the colored divider.

General Instability of Circumferentially Stiffened Sandwich Shells Subjected to Uniform External Pressure

Introduction

CELLULAR sandwich shells are preferred for many underwater applications because of their ability to withstand great hydrostatic pressures. The cellular sandwich shell, sometimes referred to as a circumferentially stiffened sandwich shell, consists of two concentric cylinders joined by a series of equally spaced circumferential annular stiffeners (Figs. 1 through 4). On the basis of theories postulated by some authorities (1,2),* it appears that cellular sandwich shells possess the highest pressure-to-weight ratio and thus represent the optimum design for pressure vessels subjected to external hydrostatic pressure. However, the advantages of this design are offset by the lack of design data for accurately predicting the hydrostatic-pressure capability of the shell. There is a need for a simple equation that will accurately predict the hydrostatic collapse pressure of the cellular sandwich shell.

PURPOSE OF THE INVESTIGATION

Cellular sandwich shells, like other types of shells, are subject to two broad categories of shell failure: elastic instability, and failure of the material. Of the two types of failure, elastic instability is less predictable and thus of greater interest. There are many types of elastic instability, but this investigation was concerned with general instability - a type of elastic failure in which all the shell components buckle simultaneously. It was the purpose of this investigation to theoretically and experimentally develop a simple equation for predicting the general-instability collapse pressure of a cellular sandwich shell subjected to hydrostatic pressure.

HYPOTHESIS AND METHOD OF INVESTIGATION

The theoretical basis of this investigation was Bresse's theory for the buckling of rings under radially applied external pressure(3). It is postulated that a modified Bresse equation accurately predicts the uniform external pressure at which general-instability failure of a cellular sandwich shell occurs. The advantages of cellular sandwich shell construction were determined by tests in which five types of acrylic resin shells were imploded (Figs. 3 and 5 through 8). To verify the validity of the modified Bresse equation, two identical aluminum cellular shells and one acrylic resin cellular shell were imploded in a carefully controlled pressurization system. Both types of shells were designed to collapse by general instability, and their collapse pressures were then compared with those predicted by the modified Bresse equation. The criterion by which the validity of the modified Bresse equation was judged is its ability to predict collapse pressure within 10 per cent of the experimental results.

This investigation was limited to the collapse of cellular sandwich shells by general instability, and only those shell parameters and experimental data that have direct bearing on this method of

*Numbers in parentheses refer to References on p. 13.

collapse were investigated. However, local buckling of sandwich-shell facings and circumferential stiffeners is discussed in a general way.

BRIEF SUMMARY OF RESULTS AND CONCLUSIONS

The two aluminum shells were tested together, and collapsed at 2300 psi; the acrylic resin shell collapsed at 1650 psi. When both collapse pressures were corrected for end conditions and compared with those obtained by the modified Bresse equation, the difference was less than 5 per cent. On the basis of this and other investigations, it is concluded that the modified Bresse equation accurately predicts the general-instability collapse pressure of cellular sandwich shells, provided the proper corrections for end conditions are made.

Theoretical Consideration and Discussion

STRUCTURAL ANALYSIS OF THE CELLULAR SANDWICH SHELL

The derivation of an equation describing the safe load of a novel structure can generally be approached from two diametrically opposite viewpoints. One viewpoint is based on the supposition that an equation describing the safe load for any new structure can be derived from the basic tenets of statics and from the theory of elasticity, providing that a thorough analysis of the distribution of loads and boundary conditions has been made previously. The other viewpoint is based on the supposition that any new structure can be considered as a combination of several structural elements for which load-carrying capabilities already have been obtained.

If an approach to the solution of a problem could be characterized by one word, the first viewpoint might be called scientific and the second, engineering. Both viewpoints have their value, depending on the aims of the investigation. The scientific formula derivation has its value when the aim of the investigation is the discovery of a basic set of equations. However, when the aim of the investigation is applicable to a specific engineering structure only, the engineering approach is much more desirable since the emphasis is on the utilitarian value of the formula and not on its value as a contribution to the theoretical body of knowledge.

As this investigation was initiated to acquire an engineering design formula for the prediction of a particular mode of failure of a special type of structure, it was decided at the very outset that only the engineering approach was desirable. This decision was further substantiated by other reasons, such as limited funds and a short period of time in which to conduct the investigation.

DEFINITION OF TERMS

The terms used in this report are defined below. Some of the structural members (such as I rings and I-ring flanges) do not exist as such, but are referred to for purposes of analysis. The cellular sandwich shell, for instance, can be thought of as concentric cylinders joined by annular stiffeners; or as a series of wide-flange I beams formed into rings, the flanges of which form the inner and outer cylinders (Fig. 2).

Annular Stiffeners - Rings joining the outside and inside shell facings to form an integral structure (Fig. 2).

Shell Facings - Thin shell-like cylinders joined by annular stiffeners (Fig. 2).

I Ring - A wide-flange I beam rolled into a circular shape (Fig. 2).

I-Ring Flange - That portion of the I beam forming the inside and outside facing of the shell (Fig. 2).

I-Ring Web - That portion of the I beam supporting the flanges.

Pressure-to-Weight Ratio - An arbitrary ratio for the comparison of various shells subjected to internal or external pressure. This comparison index takes into account both the strength-to-

weight ratio of the structural material and the buckling resistance of the shell design. The ratio is defined as:

$$\eta = P_{ce}\left(\frac{V_i}{W_i}\right),$$

where

P_{ce} = the experimentally determined hydrostatic collapse pressure of the shell,

V_i = displacement volume of the vessel per unit shell length ($in.^3$ per in.),

and

W_i = weight of the shell per unit length (lb per in.).

Hydrostatic Pressure - External pressure of uniform magnitude applied both axially and radially to the enclosed pressure vessel.

Collapse Pressure - External hydrostatic pressure that causes the pressure vessel to lose its structural integrity.

Infinitely Long Pressure Vessel - Pressure vessel possessing bulkhead spacing such that any further increase in the spacing will not decrease the collapse pressure of the vessel.

Short Pressure Vessel - Pressure vessel whose collapse pressure depends to some extent on the reinforcing action of the bulkheads.

Failure by General Instability - Type of failure in which all the structural components of the shell fail simultaneously by buckling.

General Instability Equation - Bresse's theory for the buckling of rings adapted for the calculation of the external hydrostatic pressure at which an infinitely long cellular sandwich shell will collapse because of general instability.

APPLICATION OF BRESSE RING-BUCKLING EQUATION

The sandwich shell, when analyzed structurally, can be thought of as either an assembly of typical wide-flange I rings, or as outer and inner cylinders joined by circumferential annular stiffeners at regular intervals. Although equations describing the general-instability collapse of smooth shells and circumferential rings exist, the structural interaction between these shell components is such that the general-instability collapse pressure of the assembly is not necessarily equal to the sum of the individual collapse resistances of the components. Thus, for the engineering type of investigation, it is fruitless to pursue the structural analysis approach, which treats the shell as a combination of inner and outer smooth cylinders joined by annular stiffeners. The method that logically promises a solution to the problem is the one in which the shell is considered to be made up of infinitely repeatable wide-flange I rings (Fig. 2).

When the hypothesis is made that the shell is only a series of wide-flange I rings, then it follows that the over-all collapse resistance of the shell to external pressure is equal to the buckling resistance of the structural module, the wide-flange I ring. Therefore, the over-all collapse resistance of the shell can be determined if the buckling strength of a single wide-flange I ring is known. Fortunately, the problem of ring stability under uniform, radially applied, external loading was solved long ago by Bresse(3); the solution was then extended into the plastic strain regions by Engesser(4). The difference between the loading of Bresse's ring and that of the typical shell I ring being investigated is in the superimposition of axial load upon the ring along its outer and inner flanges.

The expression for the uniformly applied radial loading that produces radial buckling of the ring has been very lucidly presented by Timoshenko(5), and his notation is used in deriving the general-instability equation for the cellular sandwich shell. This equation actually represents a semiempirical adaptation of the Bresse ring-buckling theory(3) to the buckling of sandwich shells

by general instability. The adaptation is performed on the basis of structural similarity, and the validity of the adaptation is supported by experimental data.

BUCKLING OF A CELLULAR SANDWICH SHELL UNDER HYDROSTATIC PRESSURE

In the original Bresse ring-buckling equation,

$$q_{ct} = \frac{3EI}{R^3} , \qquad 1$$

where

q_{ct} = the radial external collapse pressure of the ring (lb per in. of circumference measured along the neutral axis of the ring),

E = modulus of elasticity in compression (psi),

I = moment of inertia of the ring ($in.^4$),

and

R = radius of the neutral axis of the ring (in.).

The Bresse equation is correct for only a single ring under radially applied external pressure. This means that there is no loading perpendicular to the plane of the ring and no external restraint on the buckling ring. When shells of typical wide-flange I rings are considered, it becomes apparent that the flanges of an individual I ring are restrained from distortion by the adjacent I rings, and that they are subjected not only to radial loading but also to axial loading. The restraint on I-ring flanges and the superimposed axial loading must be accounted for in some manner; otherwise, erroneous answers will be obtained from Eq. 1.

The simplest approach to the problem of restraint on the flanges of an I ring by neighboring I rings is to assume that the cross sections of the I rings will not become distorted during compression because the adjoining flanges will prevent them from distorting. This assumption is basically the same as that made for the derivation of the buckling formula of an infinitely long smooth shell subjected to uniform external radial pressure(6). Since the cross section of the flanges will not be distorted during the compression of the rings under load, a new expression(5) must be substituted for the modulus of elasticity in Eq. 1. Thus, $E/1-\mu^2$ is substituted for E in Eq. 1, giving a new expression:

$$P_{ct} = \frac{3EI}{R^3} \times \frac{1}{1-\mu^2} \times \frac{R}{R_o} , \qquad 2$$

where

P_{ct} = the external hydrostatic collapse pressure of the shell assembly,

R_o = external shell radius,

and

μ = Poisson's ratio in the elastic range of the material under uniaxial compression.

The factor R/R_o is used to correct for the large difference between the outside shell radius and the radius of the neutral axis of the ring. For thin-walled smooth shells, such a correction is not necessary; but, for thick-walled shells, or for sandwich shells whose ratio of ring depth to ring

external surface radius is greater than 0.1 ($h/R_o > 0.1$), such a correction is mandatory because it generally amounts to approximately 10 per cent of the uncorrected value of P_{ct}. Even with the correction, Eq. 2 is not exactly correct since the flanges of the I rings do not constitute the whole I ring but only a part of it. However, a detailed correction of Eq. 2 is not necessary: a comparison of the inertias of the web and the flanges shows that the contribution of the web to the moment of inertia of the I ring is very small.

In the derivation of Eq. 2, it was assumed that the ring material followed Hooke's law faithfully from zero stress to the moment of buckling. There are very few materials that behave in such a manner; therefore, the equation must be modified to account for materials that do not follow Hooke's law. Engesser(4) and Southwell(7) have developed expressions that allow for the deviation of materials from Hooke's law and yet predict the buckling of structural members.

The Engesser solution must be used to calculate the general-instability collapse pressure of a ring or cylinder fabricated from aluminum. For the buckling of structures fabricated from materials not having linear stress-strain properties, the Engesser solution substitutes the tangent modulus of elasticity for the modulus of elasticity in Eq. 2. Little experimental data have been found on the correctness of the Engesser solution as applied to the collapse of shells or rings, but some data have been accumulated on its application to the buckling of slender rods, as shown in Fig. 9. This figure shows that the experimental points follow the theoretical curve predicting the buckling of slender rods. Since the buckling of both rods and shells is based on similar structural parameters, it is felt that the Engesser solution will hold equally well for shells and composite shells.

Equation 2 can be further refined by substitution of μ_s for μ since μ_s is Poisson's ratio of the shell material at a given stress level. In the elastic strain region, Poisson's ratio changes very little with the increasing stress level; but, in the plastic strain region, Poisson's ratio increases considerably as compared to its value in the elastic strain region. When μ_s is used instead of μ in Eq. 2, the magnitude of the calculated collapse values for the plastic strain region may increase by as much as 18 per cent(8). The difficulty in applying this correction is the scarcity of published data on the change of μ_s with the change in the stress level; thus, μ is usually used instead of μ_s. By not using μ_s, some of the calculated collapse-pressure values are placed in error; but, since it makes the calculated values smaller, it is accepted as a safe and conservative practice.

Although specifically derived for radial loading of rings, Eq. 2 can also be used to predict the general instability of cellular sandwich shells under the joint action of axial and radial external pressures. The applicability of Eq. 2 to cellular sandwich shells subjected to radial pressure, or to combined axial and radial pressures, is based on the fact that buckling in a smooth cylinder requires a much greater axial pressure than a radial pressure or combined axial and radial pressures(9). Since the axial and radial external pressures are of equal magnitude in the hydrostatic loading of a shell, the cylinder will become unstable because of radial pressure long before buckling because of axial pressure will occur. Although this has been proved experimentally and theoretically for smooth cylinders only, it is assumed that it will also apply to sandwich shells because of the similarity of the relevant shell parameters.

The final version of the Bresse ring-buckling equation, modified to include the tangent modulus of elasticity in compression E_t, Poisson's ratio at a given strain level μ_s, and the correction factor R/R_o, can be now written as

$$P_{ct} = \left(\frac{3I_{nx}}{R^3}\right)\left(\frac{1}{1-\mu_s^2}\right)\left(\frac{R}{R_o}\right)E_t \,, \qquad 3$$

where

$$I_{nx} = \frac{\left[\frac{h^3-(h-t_o-t_i)^3}{12}\right]L_r + \frac{(h-t_o-t_i)^3 t_w}{12}}{L_r} \,,$$

h = over-all wall thickness, t_o = outside flange thickness, t_i = inside flange thickness, L_r = annular stiffener spacing, and t_w = annular stiffener width. Equation 3 will be used to calculate the general-instability collapse of sandwich shells.

When the shell material has a definite yield point and becomes plastic without strain hardening, Engesser's solution does not apply; Southwell's modification(7), or some other modification, must be applied. Since this investigation does not concern itself with shells fabricated from such materials, these modifications to the Bresse equation will not be discussed.

Experimental and Testing Procedures

ACRYLIC RESIN SHELLS

Five inexpensive acrylic resin shells were constructed to determine the relative merits of the different types of shell construction. These shells, shown in Fig. 3 and Figs. 5 through 8, were of identical weight, length, outside diameter, and usable inside diameter. They were fabricated from commercially available tubes, and their rings were cut from commercial acrylic resin sheet stock. All the structural components were joined into a single homogeneous structure with acrylic resin solvent. To eliminate residual stresses introduced by machining and bonding of the material, the finished shell assemblies were annealed in temperature-controlled ovens. Figure 10 is an assembly drawing of the acrylic resin shells.

For implosion testing, the shell ends were sealed with identical friction-type closures and immersed in a 2000-psi-capacity pressure chamber (Fig. 11). The collapse pressures for all the shells were carefully recorded, and are presented in Table I. The results indicate that, among those tested, cellular sandwich construction is the best method of stiffening shells against external pressure.

TABLE I

COLLAPSE PRESSURES OF ACRYLIC RESIN SHELLS

Description*	Collapse Pressure** (psi)	Pressure-to-Weight Ratio $\eta = P_{ce}\left(\frac{V_i}{W_i}\right)$
Smooth shell	590	0.585×10^5
Smooth shell stiffened by equally spaced circumferential plain rings	1200	1.185×10^5
Smooth shell stiffened by equally spaced circumferential T rings	1450	1.44×10^5
Longitudinally stiffened sandwich shell	1100	1.09×10^5
Cellular sandwich shell	1650	1.63×10^5

*Material properties are shown in Fig. 31.
**Pressurization rate: 20 psi per sec.

ALUMINUM CELLULAR SANDWICH SHELLS

Equation 3 was used to design two larger aluminum cellular sandwich shells (models A and A') to test the general-instability collapse theory postulated. The shells were constructed of wrought aluminum, a typical construction material, which was selected solely on the basis of cost and ease of fabrication. Since engineering design formulas for this type of shell were not available at that time, both the shell facings and the rib spacing were selected on the basis of general engineering stability principles(10, 5). The thickness of the shell facings and the spacing of the ribs were critical and were selected so that local buckling(11) or yielding would not occur before the shell collapsed as a whole under the action of external pressure. Figure 12 is the assembly drawing for the aluminum cellular sandwich shells.

Since so many variables enter into the design of a sandwich shell, it is not prudent to accept the experimental collapse pressure of a single shell as the typical collapse pressure of that sandwich shell design. The best approach would be to test as many shells of the same design as possible and to evaluate the collapse pressures by statistical methods, but such an approach would be too expensive for this investigation. To overcome this limitation and to obtain at least a semblance of a typical collapse pressure, it was decided to make both aluminum shells of identical dimensions and to average their collapse pressures. The dimensional tolerances for the fabrication of both shells were very "tight," as indicated in Fig. 12. These tolerances ensured that the shells would be as nearly identical as possible and that they would collapse simultaneously during testing.

During the fabrication of the shells, all conceivable quality controls were instituted and adhered to in order to make certain that the final product tested was the same as that described in Fig. 12. The shell design demanded an unusually high degree of attention to manufacturing details on the part of the contractor - details that are generally ignored in everyday shop practice. The welding fabrication method, in particular, presented more than the usual problems.

Because of the extreme length of welds, and the required postweld heat treatment, the wrought aluminum shells required special care to avoid residual-stress distortions. Only by the use of elaborate welding jigs and uniform welding rates was it possible to keep the distortion of the shells within the design specifications. The most important single item in the structural strength of the wrought aluminum shells was the quality of the welds, which was so high that it surpassed the fabrication specifications by 21 per cent, as shown in Table II.

Another important item in the design and fabrication of these shells was the location of the welds. Actually, there are several ways in which shell components can be joined to form a welded shell structure; the selection of the weld type and its location depends primarily upon the stresses created by external pressure application. Since external pressure loading generates the greatest stresses in the circumferential direction, the welds had to be located along the circumference of the shell; but, even at this location, there were several alternatives for the selection of weld type and placement.

After a careful evaluation of all the possible weld types and locations, a weld was selected that would be almost as strong as the parent material, provided it was properly applied and located. This weld, which is shown in Fig. 12, was placed in the circumferential direction and joined the flanges of individual wide-flange I rings.

Each of the shells was provided with a wedge-band joint at each end for coupling with another shell of identical construction. The joints were equipped with standard neoprene O rings in a radial-type sealing arrangement that effectively sealed the shell assembly against high external testing pressures.

TEST APPARATUS AND SHELL END SUPPORTS

The basic apparatus required for implosion testing consisted of two shell end closures, an internal pressure vessel, a hydraulic pump, and several accurate pressure indicators. At the time this investigation was conducted, the Ordnance Research Laboratory did not have pressurizing equipment of sufficient capacity to test the two aluminum experimental shells. All experimental testing of the aluminum shells was performed at the Southwest Research Institute, San Antonio, Texas.

TABLE II

MATERIAL PROPERTIES OF COLLAPSED ALUMINUM SHELLS

Test Sample	No.	Cross Section ($in.^2$)	Elongation in 1 In. (per cent)	Load (lb)	Ultimate Strength (psi)
Parent material	1	0.0986	17.47	4765	48,327
	2	0.095	19.50	4650	48,947
Weld coupon	1	0.1005	4.42	4010	39,900
	2	0.1003	3.90	4005	39,930
	3	0.0995	5.18	4200	42,211
	4	0.102	4.06	4110	40,294
	5	0.0997	3.68	3910	39,218
	6	0.1003	4.60	4045	40,329
	7	0.101	4.08	3855	38,168
	8	0.1005	4.46	4260	42,388
	9	0.1005	4.89	4180	41,592
	10	0.1005	4.89	4165	41,443

Material and Construction

Parent material - 6061-T6 aluminum alloy
Welds -
Root pass: 5356 filler, heliarc-welded
Filler passes: 4043 filler, Sigma-welded
Weld type - 90-deg single-vee butt weld

Material Strengths

Specified weld strength - 33,500 psi (see Fig. 12)
Average weld strength - 40,547 psi; 83.5 per cent of average parent material strength
Specified parent material strength - 42,000 psi (see Fig. 12)
Average parent material strength - 48,637 psi

Test Description

Method of testing - tensile
Strain rates - 0.001 in. per sec

The method of mounting the shells inside the tank requires careful consideration. Depending on the type of shell support inside the tank, the experimental collapse of a given shell will vary anywhere from 5 to 500 per cent of an infinitely long shell collapse pressure. These percentages depend on the shell's ratio of ring depth to mean diameter (h/D) and its ratio of length to mean diameter (L/D).

There are four types of shell end supports: rigid, simple, friction, and elastic (Fig. 13). Each type of end support imposes a different shell end condition, which, in turn, usually changes the experimental collapse strength of the shell. There is, generally speaking, no one preferred type

of shell support; they all have their value, depending on what the testing arrangement is supposed to simulate. For this investigation, the friction type of end support was selected.

Shells are classified as infinitely long when their dimensions are such that a further increase in length will not change their collapse pressure. Shells of interest to the Laboratory - that is, shells whose L/D ratio is greater than 5 and whose h/D ratio is between 0.1 and 0.05 - are considered to be infinitely long shells.

Two approaches to shell testing are possible: the most straightforward, but more expensive, approach requires experimental shells whose bulkhead lengths are more than five times their diameters (L>5D) and whose ends are rigidly or simply supported; and a less accurate, but also less expensive, approach that uses shorter shells equipped with friction end supports to simulate the collapse strength of longer shells (L>5D).

The reasoning behind the second approach is based on the assumption that the collapse resistance (psi of external pressure) of a short shell is actually the collapse resistance of an infinitely long shell stiffened by the presence of friction end supports at each end of the shell. The stiffness of the end rings, and the friction between the end rings and the closure plates, are calculable; their effect on the shell collapse strength can be subtracted from the over-all short sandwich shell collapse pressure - the end result being the collapse pressure of a long sandwich shell. This type of end support was used for the testing of both the small-scale acrylic resin shells and the large aluminum shells. The stiffness of the end rings, and the friction between the end adapter rings and closure plates, were different for the two types of shells; but, in each case, the variable parameters were the same and could be calculated by the same equations.

TEST FACILITIES AT THE SOUTHWEST RESEARCH INSTITUTE

Pressurization System. The pressure tank in which the implosion testing of the shells was conducted (Fig. 14) is located at the Mechanics Laboratory of SRI. The dimensions of the tank are 30 in. in diameter by 150 in. long, and it is able to safely contain pressures up to 10,000 psi. The tank is actually composed of a section of straight thick tube threaded internally at both ends and capped with solid steel discs. The sealing between the discs and the tube is accomplished by standard O rings backed with steel expansion rings. The cap on the loading end of the tube has an 8-in.-diameter opening that permits observation of the inside of the shell during implosion testing. The whole tank assembly is positioned inside a concrete-lined silo in the floor of the building, with the loading end of the tank being almost flush with the floor.

Instrumentation. To record the strains and deflections of the shell inside the pressure chamber, several types of instruments are available at SRI. However, electrical resistance strain gages and strain-recording equipment were used exclusively for this investigation.

For the recording of strains indicated by the strain gages, an automatic scanner-recorder was used, permitting the balancing and recording of 48 gage circuits in 1 min. The rapidity with which all the strains could be read and recorded eliminated any discrepancies resulting from creep of shell material or from creep of the adhesive with which the gages were attached to the shell.

The electrical-resistance strain gages were mounted on critical areas of the shell assembly. The location and the identification of gages are shown in Figs. 15 and 16. Since all the strain gages were mounted on the inside of the shell, only a temperature-compensating gage was required, and the pressure-compensating gage was eliminated.

TESTING PROCEDURE FOR SHELL MODELS A AND A'

Both the instrumentation and testing procedures were planned to provide the greatest amount of information possible. In addition to obtaining the collapse pressures of Models A and A', it was desirable to obtain information about the influence of end conditions on collapse pressure.

The twin shells were assembled into one pressure vessel assembly capped at both ends with friction-type end closure plates (Fig. 14). The assembly was placed inside the pressure chamber, the chamber cover was screwed down tight, and the entrapped air in the chamber was bled off to

the atmosphere. After the chamber was checked for leakage, the oil inside the chamber was pressurized to 100 psi, and all the strain gages were balanced at that pressure. The pressurizing of the oil in the tank and the recording of strains were performed simultaneously by two operators, the pump operator following orders from the strain-recorder operator. Upon command, the pump operator increased the pressure to 200 psi for the duration of the automatic scanner-recorder's strain-recording cycle. When the recording cycle was completed, the pressure was raised to 300 psi and the recording cycle was repeated. This procedure was repeated until a pressure of 1100 psi was reached.

At 1100 psi the strain recorder was disconnected and the pressure was cycled from 0 to 1100 psi 25 times. The cycling of pressure at 1100 psi eliminated any residual stresses caused by the prior welding and heat treating of the shell assembly. After the cycling was completed, the strains were recorded again in an identical manner to check for any creep or redistribution of strains that might have occurred during the repeated pressure cycling. Upon completion of the pressure-cycling, stress-relieving program, the shells were coupled in reverse order and again positioned inside the pressure chamber to obtain some strain readings at the shell assembly ends resting against the end closure plates. The comparison of circumferential strain readings at the center and ends of the shell assembly showed the influence of the end adapter rings sliding upon the end closure plates.

For the actual implosion test, the pressure was raised in 200-psi increments, and the strains were recorded at each level. The pressure increases were continued until implosion of the shell assembly occurred at 2300 psi. Both shells collapsed simultaneously, so further testing was not necessary. Figure 17 shows a collapsed shell; Fig. 18 shows the deformation of the shells after implosion.

The collapsed shells were dissected (Figs. 19 and 20), and the thicknesses of the I-ring flanges and webs were compared to the specifications (Fig. 12) to determine any possible deviations. Since the welds comprise a large amount of filler material on the shell, coupons were cut from the imploded shells and tested to destruction to determine their strength.

Experimental Results

SHELL STRAINS UNDER EXTERNAL PRESSURE

The strains recorded by the strain gages (Figs. 21 through 27) give considerable information about the behavior of the shells under load. There was no difference between the readings of the mid-bay strain gages at the beginning and end of the cycling test, so only one set of curves was plotted (Figs. 21 through 24). These curves indicate that only a negligible amount of residual stress was present; otherwise, the difference between the strains recorded at the beginning and at the end of the test would have been noticeable, indicating that some realigning of stresses had taken place. This realigning was expected because of the repeated elastic loading and unloading of the shell structure, but the results do not bear this out. There is a considerable difference between the strains at the shell mid-bays and at the shell ends, proving that individual shell ends are stiffer than the I rings.

Both shells imploded simultaneously, but the rate of deformation and the extent of damage were not the same. The strain gages at mid-bay locations did not indicate any noticeable difference in circumferential strains, but the gages located at the ends of the shells showed a difference. When the circumferential strains at the ends of the two shells were compared, it became apparent that the ends deformed at different rates and thus supplied different amounts of restraint to the shells, causing one to fail sooner than the other. The difference in the final amount of deformation can be deduced from the measurements of the outside shell diameters at different points along the length of the shell (Fig. 18). From the difference in the plastic deformation of the two shells, it is estimated that the collapse strengths of the two shells differed by 50 to 100 psi, which is less than 5 per cent of the actual experimental collapse pressure of 2300 psi.

DISSECTION OF IMPLODED SHELLS

An examination of the collapsed shell (Fig. 17) and of the dissected collapsed shell (Fig. 19) did not indicate that any local buckling occurred before total collapse by general instability. Detailed observation of the I-ring flanges and webs indicated that these members were in excellent condition. These results are of great importance, for they eliminate the need to consider the influence of local instability on the buckling by general instability. The fact that local buckling did not occur is the single most important result of this investigation. If local buckling were present, the comparison between theoretically predicted and experimentally determined collapse pressures would be difficult. As mentioned previously, the theory developed in this report presupposes only the existence of general instability unimpaired by the influence of failures caused by local buckling of material.

To determine whether the shells actually represent the shell specified in Fig. 12, accurate measurements of the I-ring flanges, webs, and web spacings were made at various locations. The measurements failed to disclose any deviation from the specifications. Coupons were cut at various locations and subjected to tensile tests in a hydraulic press (refer to Table II). Both the material and the welds were found to surpass the specification tolerances by approximately 20 per cent.

Comparison of Experimental and Theoretical Results

Figure 28 compares the collapse pressure calculated by means of Eq. 3 with the collapse pressure obtained experimentally. The corrected theoretical collapse pressure for the two shells almost coincides with the experimental collapse pressure. Figure 28 actually shows the relationship between the over-all depth of a sandwich wall and the collapse pressure, providing the cross-sectional area of the sandwich wall remains constant as the depth of the wall varies. Such a graph is especially useful in the design of sandwich shells, and was used in designing Models A and A'. Once Eq. 3 has been plotted, it is easy to select the optimum wall depth for a shell of given outside diameter, material, and weight. The optimum wall depth (denoted in calculations by h, Fig. 2) is represented by the sandwich wall that provides the most rigidity for the shell and occupies the least internal shell volume. The optimum wall depth for the aluminum shells is shown in Fig. 28 and that for the acrylic resin shell, in Fig. 29.

For the aluminum shells, a point on the graph (Fig. 28) has been selected where the rate of gain in resistance to collapse is the least and the rate of increase in the wall depth, h, is the greatest. This point is located immediately after the change-over from the linear slope to the almost horizontal slope in Fig. 28. This point also represents the shell wall depth that gives the maximum internal shell diameter. Selection of any other point on the graph will result in a shell that has considerably lower collapse pressure and slightly larger internal diameter, or in a shell that has slightly higher collapse pressure but considerably smaller inside diameter.

For the plotting of Eq. 3, it was necessary to obtain data on the behavior of both 6061-T6 aluminum alloy and acrylic resin. These data consisted of three curves: a stress-strain curve, a tangent-modulus-of-elasticity-vs-stress curve, and a Poisson's-ratio-vs-stress curve. The first two curves for 6061-T6 aluminum alloy were obtained from Alcoa Research Laboratories, and the most important one is reproduced in Fig. 30. Since a literature search failed to unearth any data on the third curve and since funds were not available to determine it experimentally, the curve of Fig. 30 was plotted by means of Poisson's ratio for zero stress level, obtained from Alcoa. It was assumed that the error introduced by this simplification is of only minor magnitude. The assumption that the error introduced by the use of μ instead of μ_s is small is based on the known change of Poisson's ratio for 2014-T6 aluminum alloy. Poisson's ratio at a given strain level of this alloy increases to 0.4 in the intermediate plastic strain region. If this ratio also becomes 0.4 for 6061-T6 aluminum alloy in the intermediate plastic strain region, failure to take this into account would introduce only a 6 per cent error in the calculated collapse pressure of the shell. The data for the determination of the tangent modulus of elasticity for acrylic resin were obtained experimentally, and are presented in Fig. 31.

When comparison is made between the theoretical and experimental collapse pressures, a distinction must be made between experimental values and corrected experimental values. The

recorded experimental collapse pressures must be corrected to take into account the reinforcement of the shell by individual shell joints, end adapter rings, and friction end closure plates. If corrections were not made for this strengthening effect, the experimentally obtained collapse values would not represent the collapse pressure of a long shell, but would represent the collapse pressure of a short section stiffened at the ends, for which Eq. 3 is not applicable. When all the end conditions were taken into account, the collapse strength of the aluminum shell assembly tested was calculated to be 380 psi greater than that of an infinitely long shell of the same design. The difference between the corrected, experimentally obtained, collapse pressure and the collapse pressure predicted on the basis of Eq. 3 is 80 psi, which is less than 5 per cent, and thus satisfactory for engineering design purposes.

The corrected collapse pressure of Fig. 28 shows very close agreement with the collapse value theoretically calculated on the basis of the modified Bresse equation (Eq. 3). However, because some of the assumptions on which the corrections are based may contain inaccuracies, the coincidence of the two values alone is not construed as absolute proof that Eq. 3 predicts the general-instability collapse pressure of a cellular sandwich shell.

Further evidence that Eq. 3 predicts the general-instability collapse of sandwich shells was obtained from calculation of the collapse pressure of the acrylic resin sandwich shell (Fig. 29) and from calculation of the collapse pressure of steel cellular shells tested by the David Taylor Model Basin(12). The experiments performed at DTMB utilized steel shells of similar sandwich construction but of different h/D ratios; and their collapse pressures, when recalculated by means of Eq. 3, also agree with the experimental collapse pressures.

When all this experimental evidence is taken into consideration, it can be stated that sufficient support exists to substantiate the hypothesis that Eq. 3 accurately predicts the general-instability collapse of cellular sandwich shells.

Summary and Conclusions

Both aluminum cellular sandwich shells collapsed at 2300 psi because of general instability. When this pressure was corrected for the reinforcing effect of joint rings and friction-type end supports, a corrected collapse pressure of 1920 psi was obtained. The corrected experimental collapse pressure of 1920 psi, when compared with the collapse pressure of 2000 psi calculated by the modified Bresse equation, shows little difference. Similar results were obtained when the corrected experimental collapse pressure of the acrylic resin cellular sandwich shell was compared with the collapse pressure calculated by the modified Bresse equation. In both cases, the accuracy of the modified Bresse equation is less than 5 per cent.

It is concluded that the modified Bresse equation accurately predicts the general-instability collapse pressure of infinitely long cellular sandwich shells. This conclusion is based on the comparison of theoretically and experimentally determined collapse pressures. Although the modified Bresse equation is intended for infinitely long cellular sandwich shells, it can also be used for short shells provided the proper corrections for end conditions are made.

The modified Bresse equation is limited to the collapse of cellular sandwich shells by general instability. However, there are many other types of shell failure that should be investigated: local buckling of ring flanges, local buckling of ring webs, or local yielding of the shell material. The greatest impediment to these investigations is the lack of well documented implosion-test data for cellular sandwich shells of different lengths and diameters. Both experimental and theoretical approaches are necessary to obtain workable design equations for cellular sandwich shells.

References

1. E. I. Grigolyuk, "Buckling of Sandwich Construction Beyond the Elastic Limit," Journal of Mechanics and Physics of Solids, Vol. 6, July 1958, pp. 253-266.

2. R. E. Fulton, "Buckling Analysis and Optimum Proportions of Sandwich Cylindrical Shells under Hydrostatic Pressure," University of Illinois, Structural Research Series No. 199, June 1960.

3. M. Bresse, Cours de Mécanique Appliquée, 3rd Ed., Paris, 1880.

4. F. Engesser, "Knickfestigkeit gerader Stäbe," Zeitschrift für Architektur und Ingenieurwesen, 1889, p. 455.

5. S. Timoshenko, Strength of Materials - Part II, D. Van Nostrand Company, Inc., New York, 1956, pp. 178-190.

6. G. H. Bryan, "Application of the Energy Test to the Collapse of Long Thin Pipe under External Pressure," Proceedings of the Cambridge Philosophical Society, London, Vol. VI, 1888, pp. 287-292.

7. R. V. Southwell, "On the Collapse of Tubes by External Pressure," London, Edinburgh, and Dublin Philosophical Magazine and Journal of Science, Vol. 25, May 1913, pp. 687-698; Vol. 26, September 1913, pp. 502-511; Vol. 29, January 1915, pp. 67-77.

8. E. Gratzel and H. Schlechtweg, "Stress Distribution in a Cylindrical Brittle Tube under Uniform Internal and External Pressure," Zeitschrift für Angewandte Mathematik und Mechanik, Vol. 34, No. 3, March 1954, pp. 81-104.

9. S. B. Batdorf, A Simplified Method of Elastic Stability Analysis for Thin Cylindrical Shells, National Advisory Committee for Aeronautics, NACA Report 874, 1947.

10. S. Timoshenko, Strength of Materials - Part I, D. Van Nostrand Company, Inc., New York, 1956.

11. R. von Mises, "Der Kritische Aussendruck Zylindrischer Rohre," Verein Deutscher Ingenieure, Vol. 59, No. 19, 1914, pp. 750-755.

12. E. E. Johnson, Structural Research on Hulls for Extreme Depth, David Taylor Model Basin, Report C-1214, September 1960.

Illustrations

Fig. 1 - Aluminum Cellular Sandwich Shell

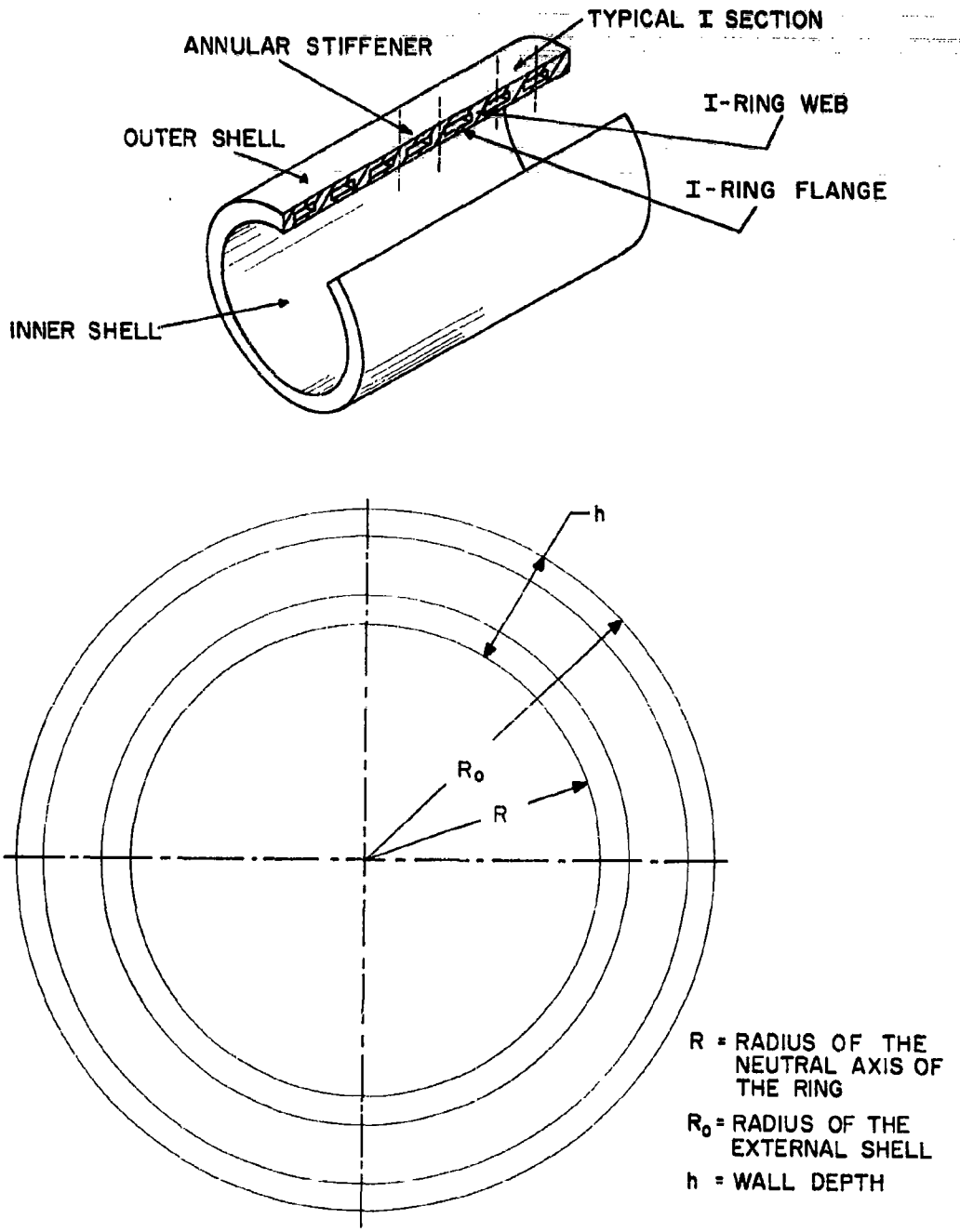

Fig. 2 - Structure of Cellular Sandwich Shell

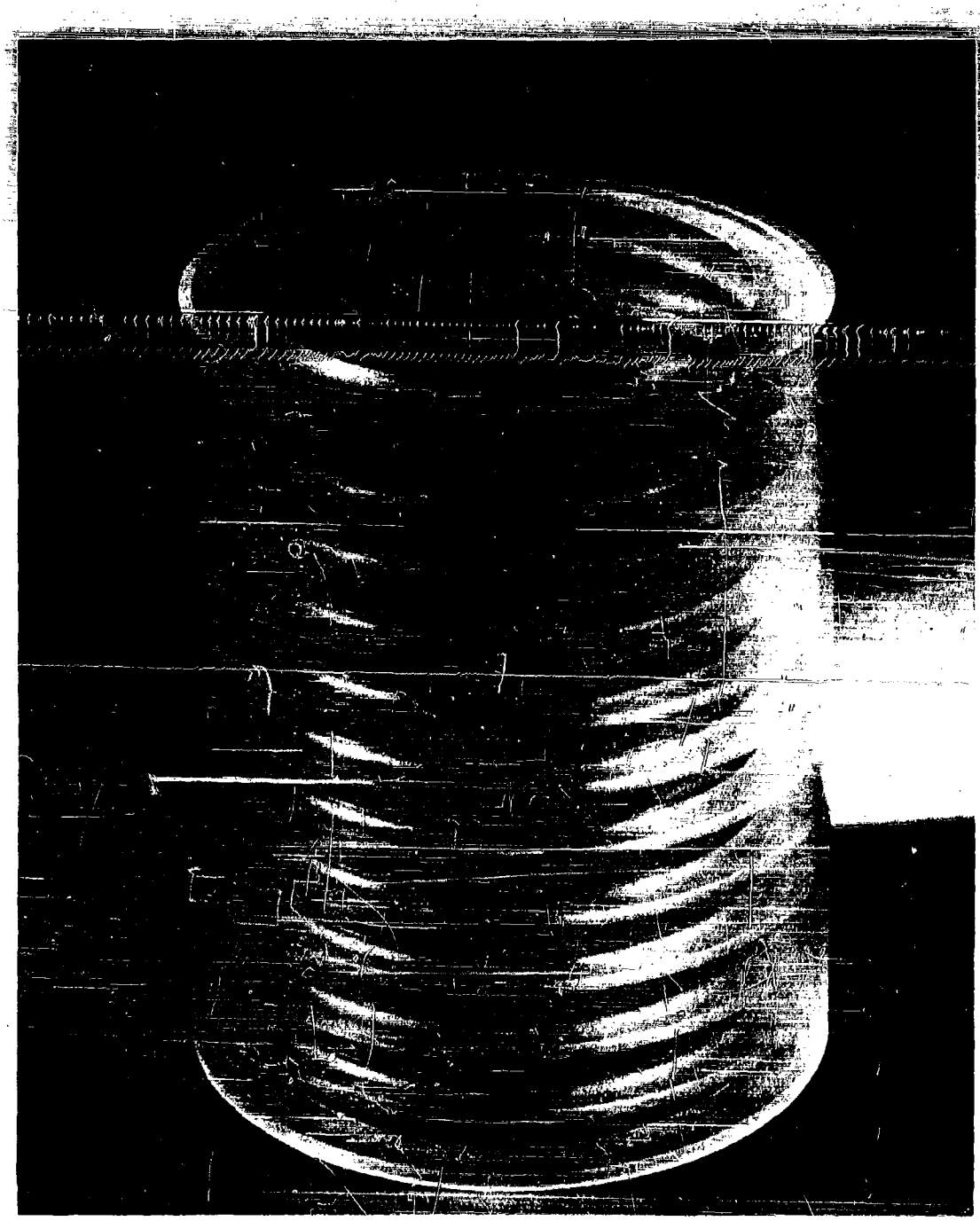

Fig. 3 - Acrylic Resin Cellular Sandwich Shell

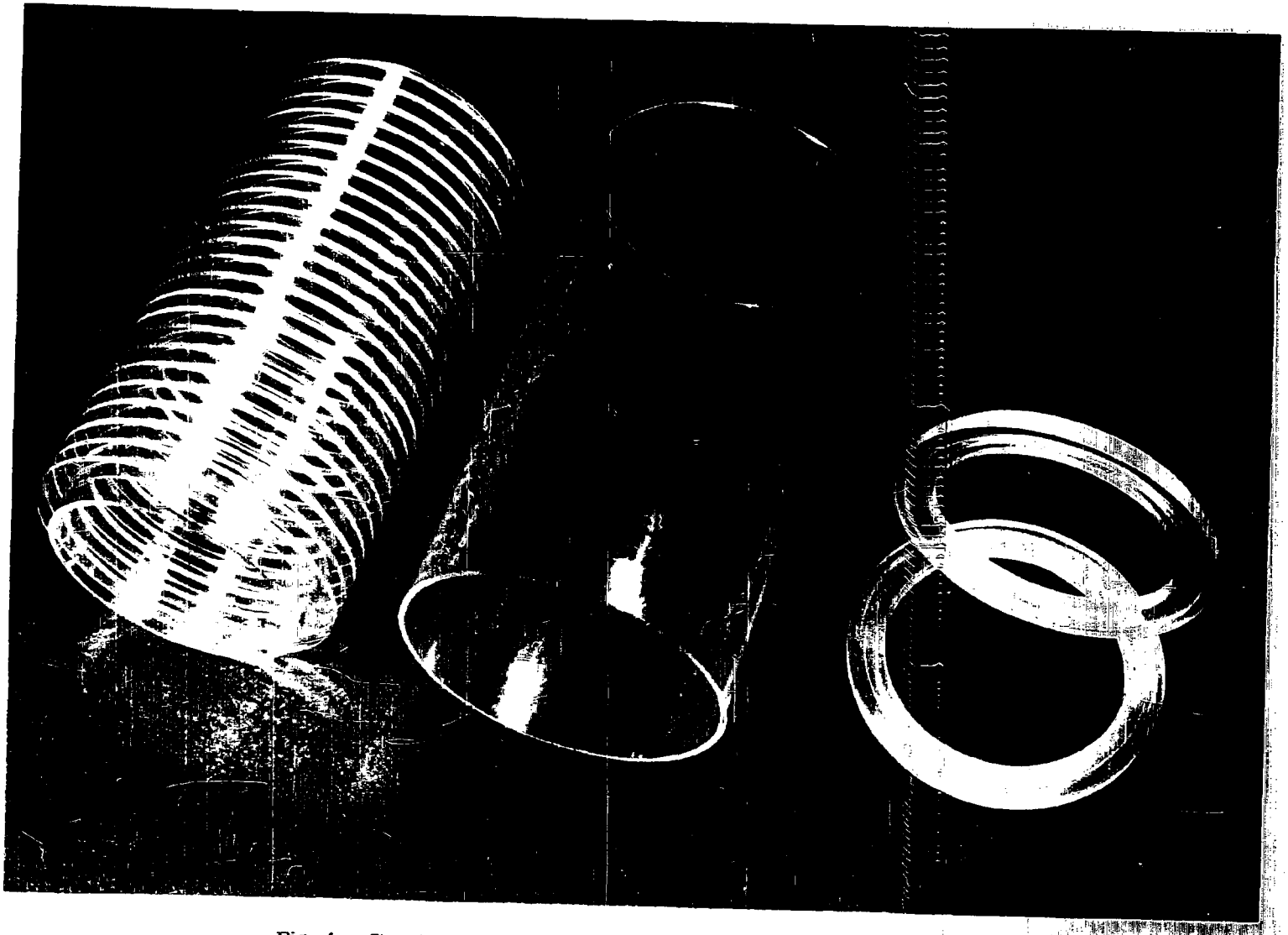

Fig. 4 - Structural Components of Acrylic Resin Cellular Sandwich Shell

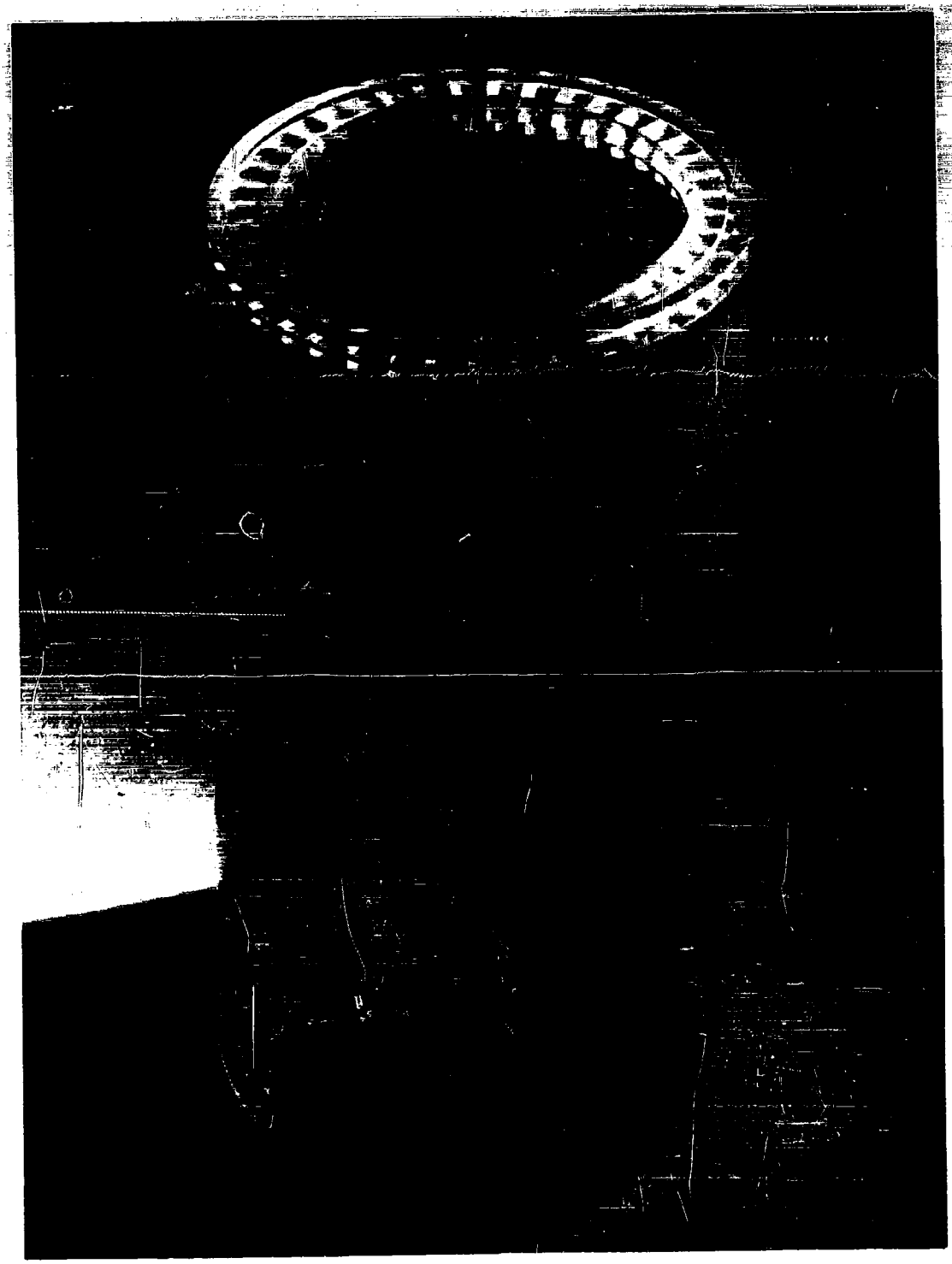

Fig. 5 - Acrylic Resin Tubular Sandwich Shell

Fig. 6 - Acrylic Resin Smooth Shell

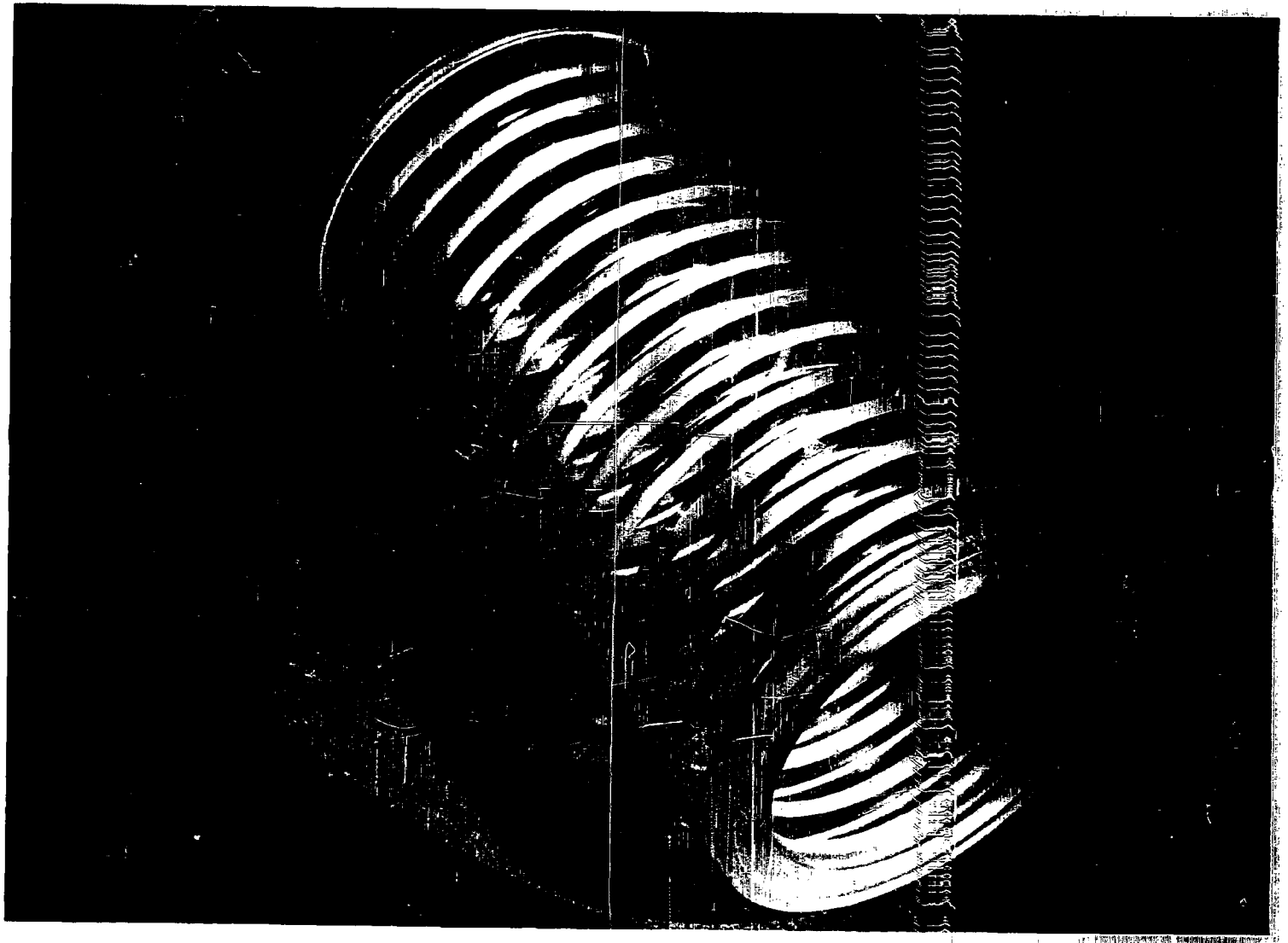

Fig. 7 - Acrylic Resin Smooth Shell Stiffened by Equally Spaced Circumferential Plain Ribs

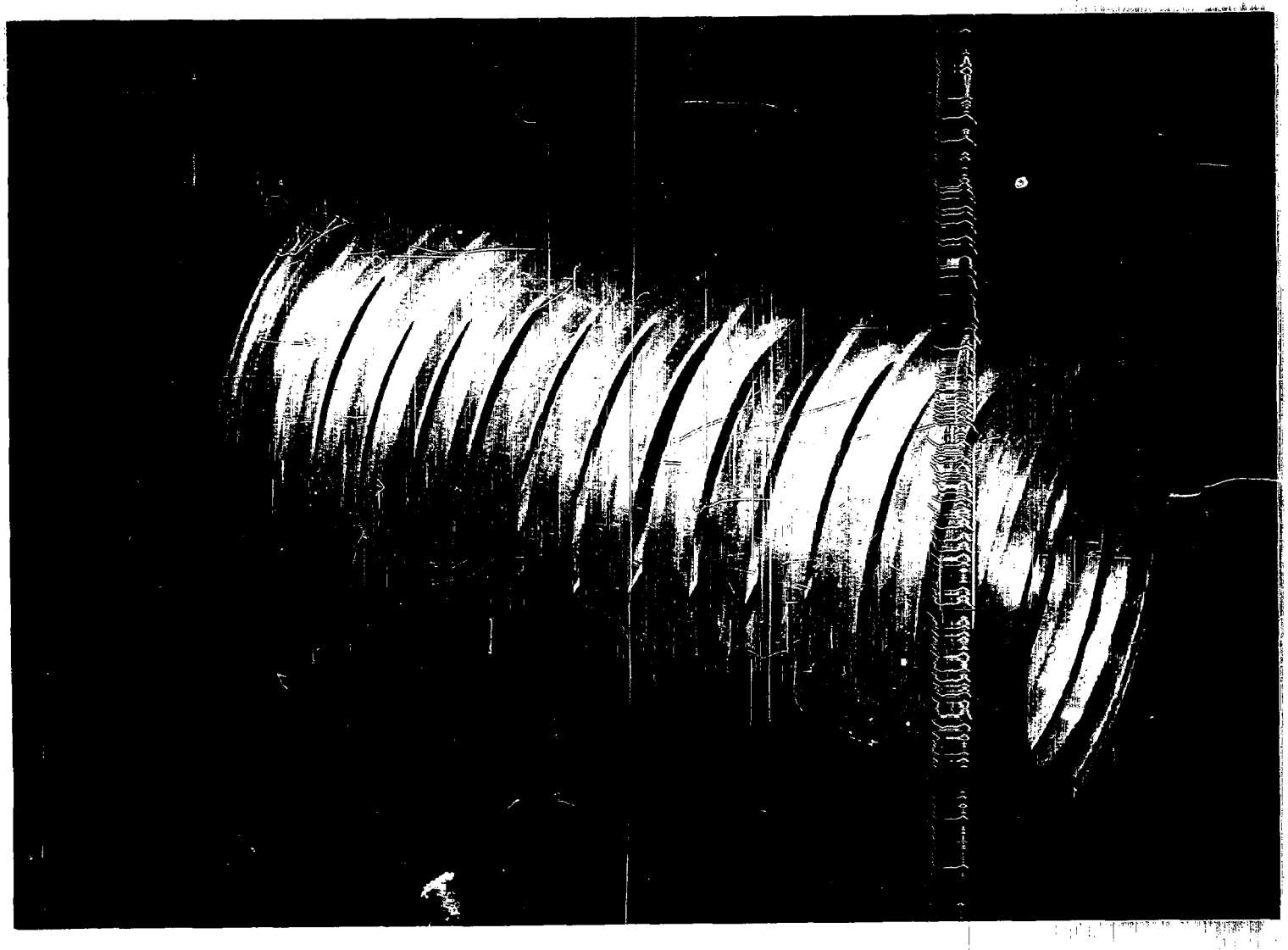

Fig. 8 - Acrylic Resin Smooth Shell Stiffened by Equally Spaced Circumferential T Ribs

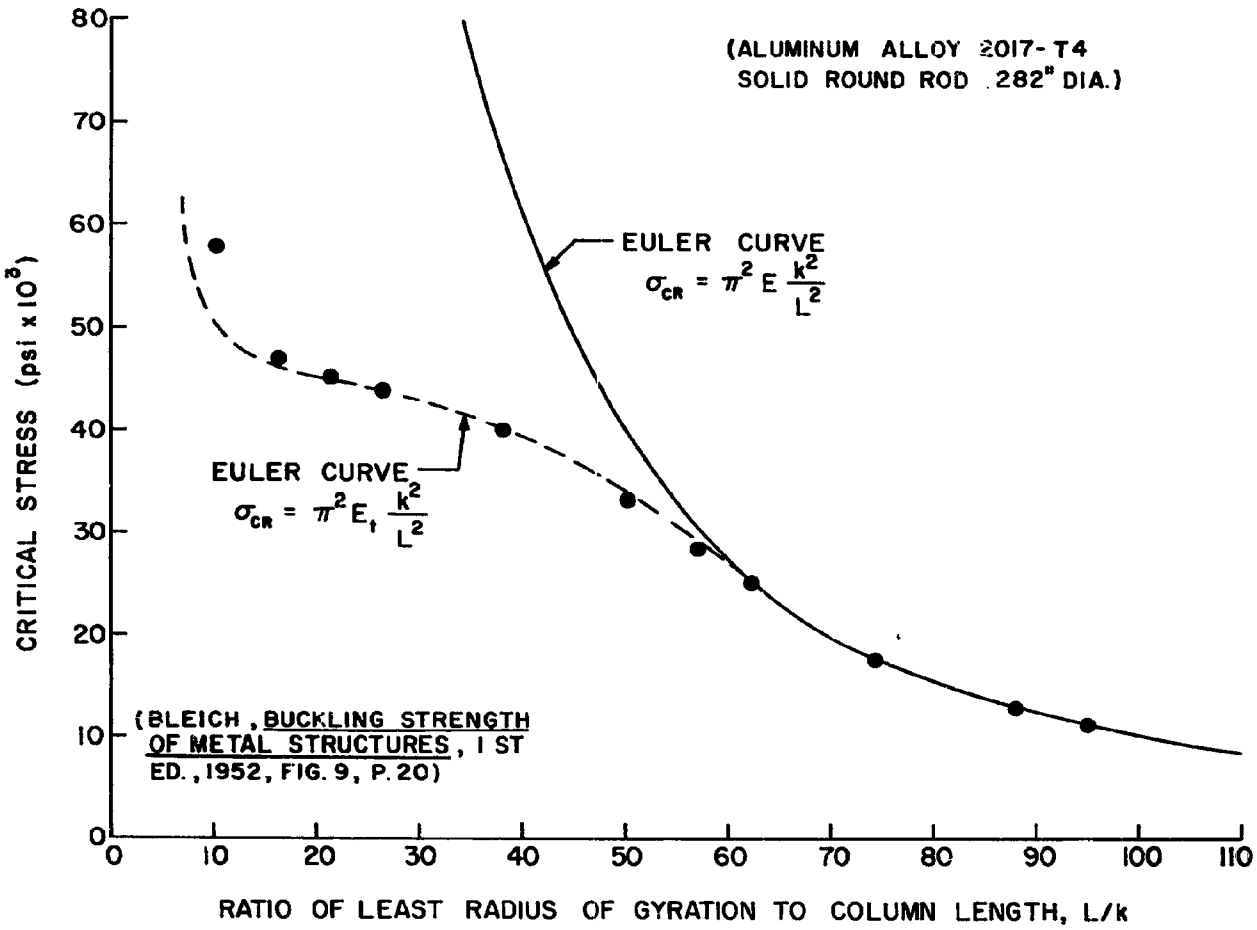

Fig. 9 - Buckling of Slender Aluminum Rods

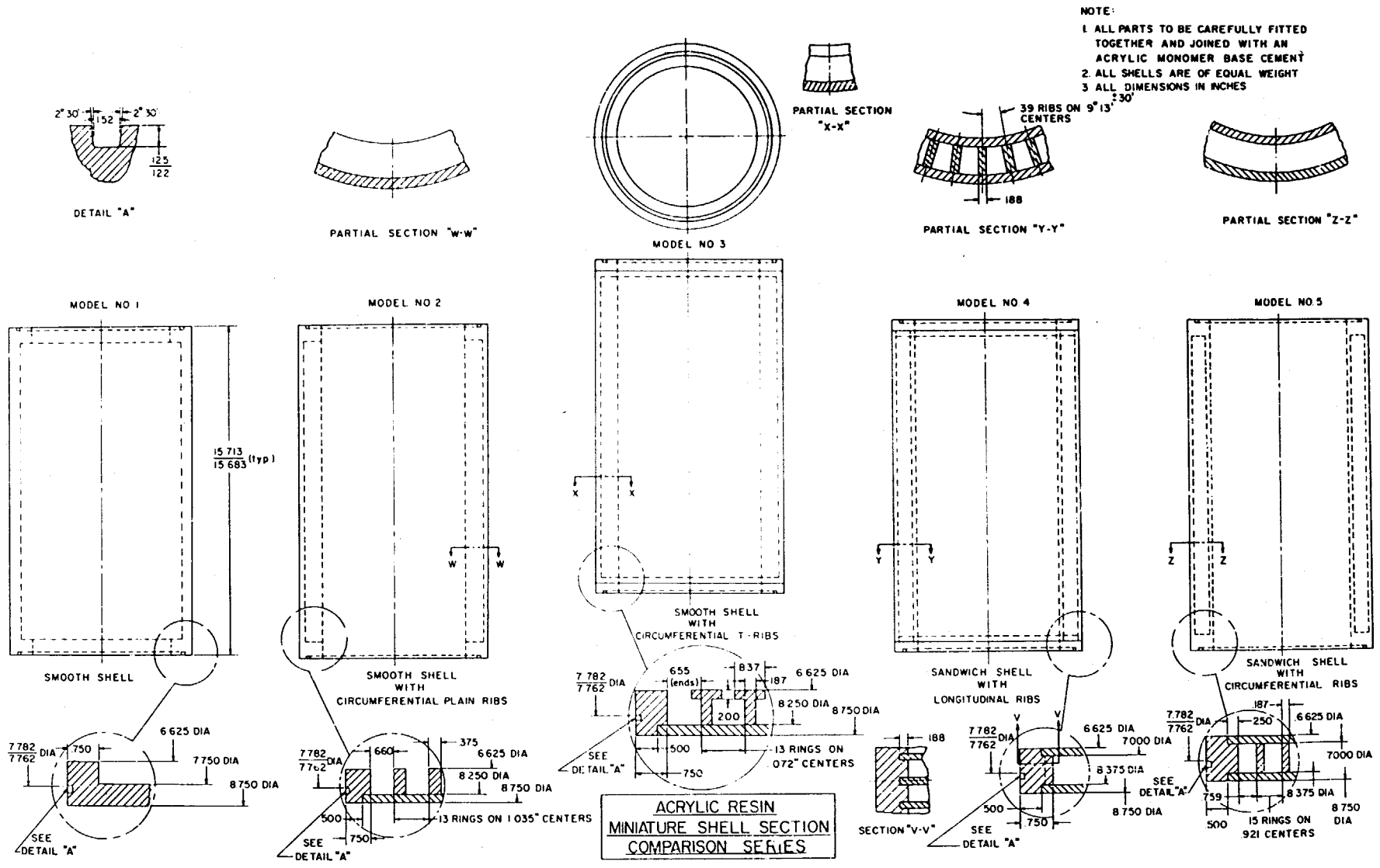

Fig. 10 - Assembly Drawing of Acrylic Resin Shells

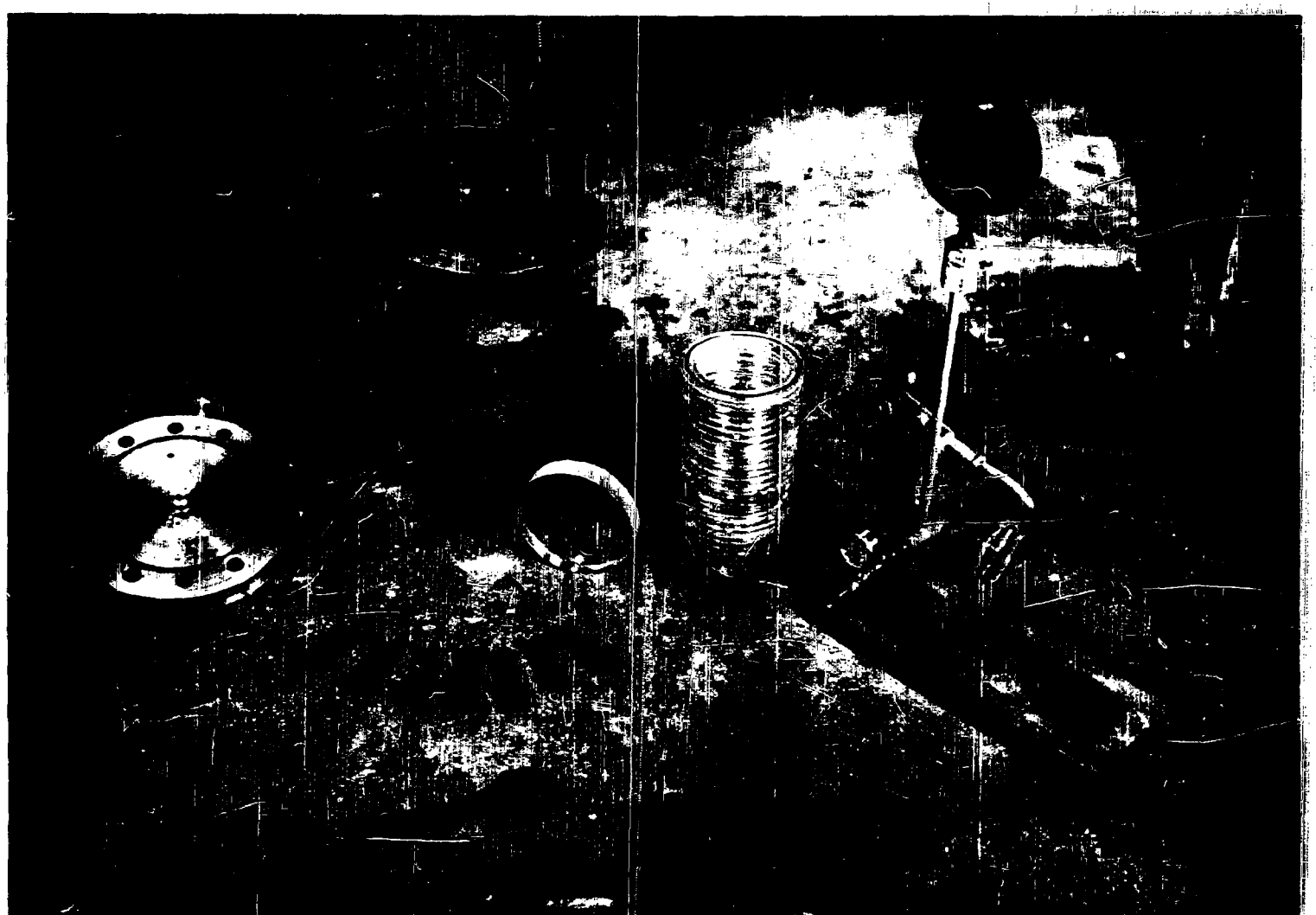

Fig. 11 - Equipment Required for Implosion Testing of Acrylic Resin Shells

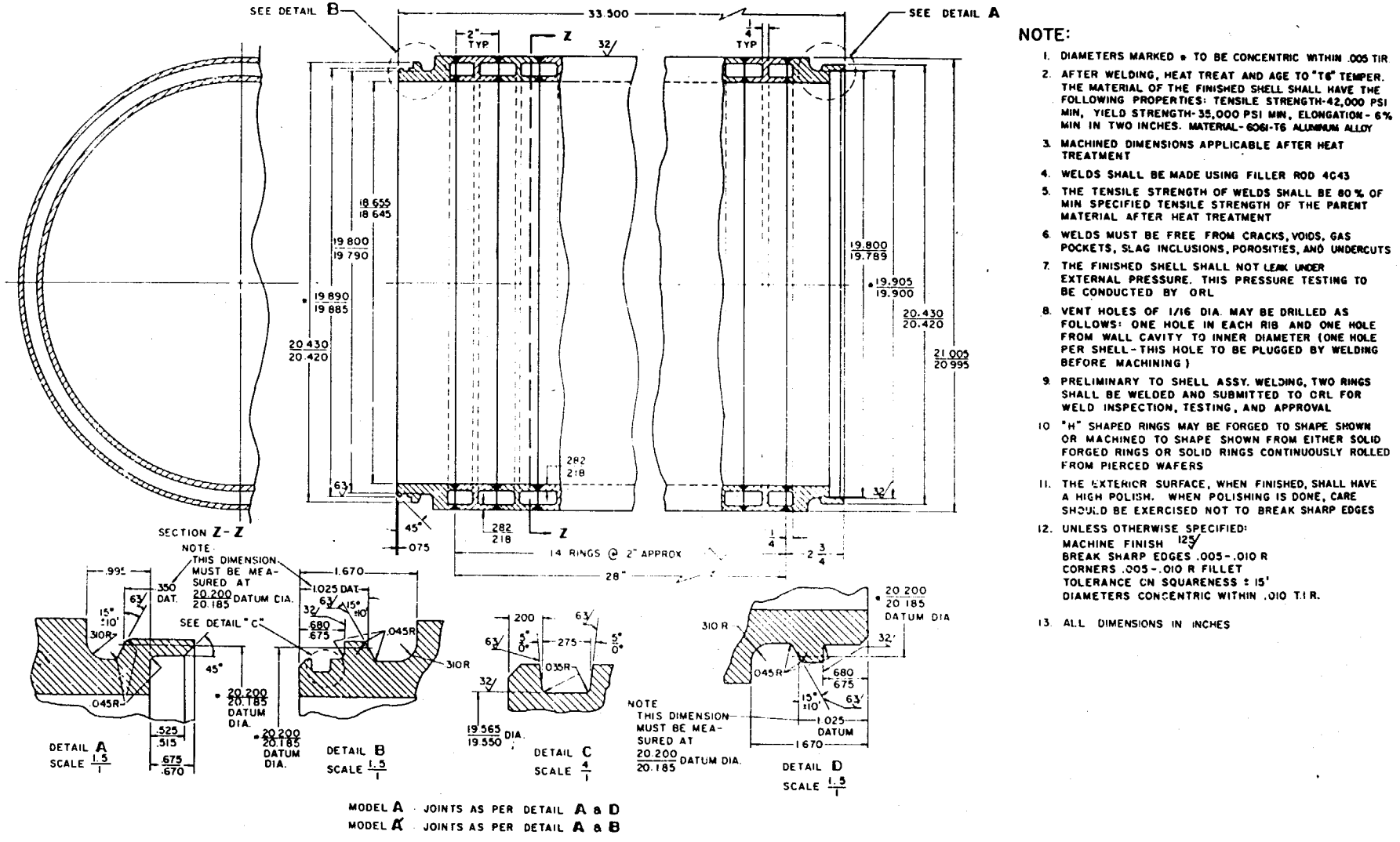

NOTE:

1. DIAMETERS MARKED ⌀ TO BE CONCENTRIC WITHIN .005 TIR
2. AFTER WELDING, HEAT TREAT AND AGE TO "T6" TEMPER. THE MATERIAL OF THE FINISHED SHELL SHALL HAVE THE FOLLOWING PROPERTIES: TENSILE STRENGTH-42,000 PSI MIN, YIELD STRENGTH-35,000 PSI MIN, ELONGATION - 6% MIN IN TWO INCHES. MATERIAL - 6061-T6 ALUMINUM ALLOY
3. MACHINED DIMENSIONS APPLICABLE AFTER HEAT TREATMENT
4. WELDS SHALL BE MADE USING FILLER ROD 4043
5. THE TENSILE STRENGTH OF WELDS SHALL BE 80% OF MIN SPECIFIED TENSILE STRENGTH OF THE PARENT MATERIAL AFTER HEAT TREATMENT
6. WELDS MUST BE FREE FROM CRACKS, VOIDS, GAS POCKETS, SLAG INCLUSIONS, POROSITIES, AND UNDERCUTS
7. THE FINISHED SHELL SHALL NOT LEAK UNDER EXTERNAL PRESSURE. THIS PRESSURE TESTING TO BE CONDUCTED BY ORL
8. VENT HOLES OF 1/16 DIA. MAY BE DRILLED AS FOLLOWS: ONE HOLE IN EACH RIB AND ONE HOLE FROM WALL CAVITY TO INNER DIAMETER (ONE HOLE PER SHELL - THIS HOLE TO BE PLUGGED BY WELDING BEFORE MACHINING)
9. PRELIMINARY TO SHELL ASSY. WELDING, TWO RINGS SHALL BE WELDED AND SUBMITTED TO ORL FOR WELD INSPECTION, TESTING, AND APPROVAL
10. "H" SHAPED RINGS MAY BE FORGED TO SHAPE SHOWN OR MACHINED TO SHAPE SHOWN FROM EITHER SOLID FORGED RINGS OR SOLID RINGS CONTINUOUSLY ROLLED FROM PIERCED WAFERS
11. THE EXTERIOR SURFACE, WHEN FINISHED, SHALL HAVE A HIGH POLISH. WHEN POLISHING IS DONE, CARE SHOULD BE EXERCISED NOT TO BREAK SHARP EDGES
12. UNLESS OTHERWISE SPECIFIED:
    MACHINE FINISH 125
    BREAK SHARP EDGES .005-.010 R
    CORNERS .005-.010 R FILLET
    TOLERANCE ON SQUARENESS ± 15'
    DIAMETERS CONCENTRIC WITHIN .010 T.I.R.
13. ALL DIMENSIONS IN INCHES

Fig. 12 - Assembly Drawing of Aluminum Cellular Sandwich Shell

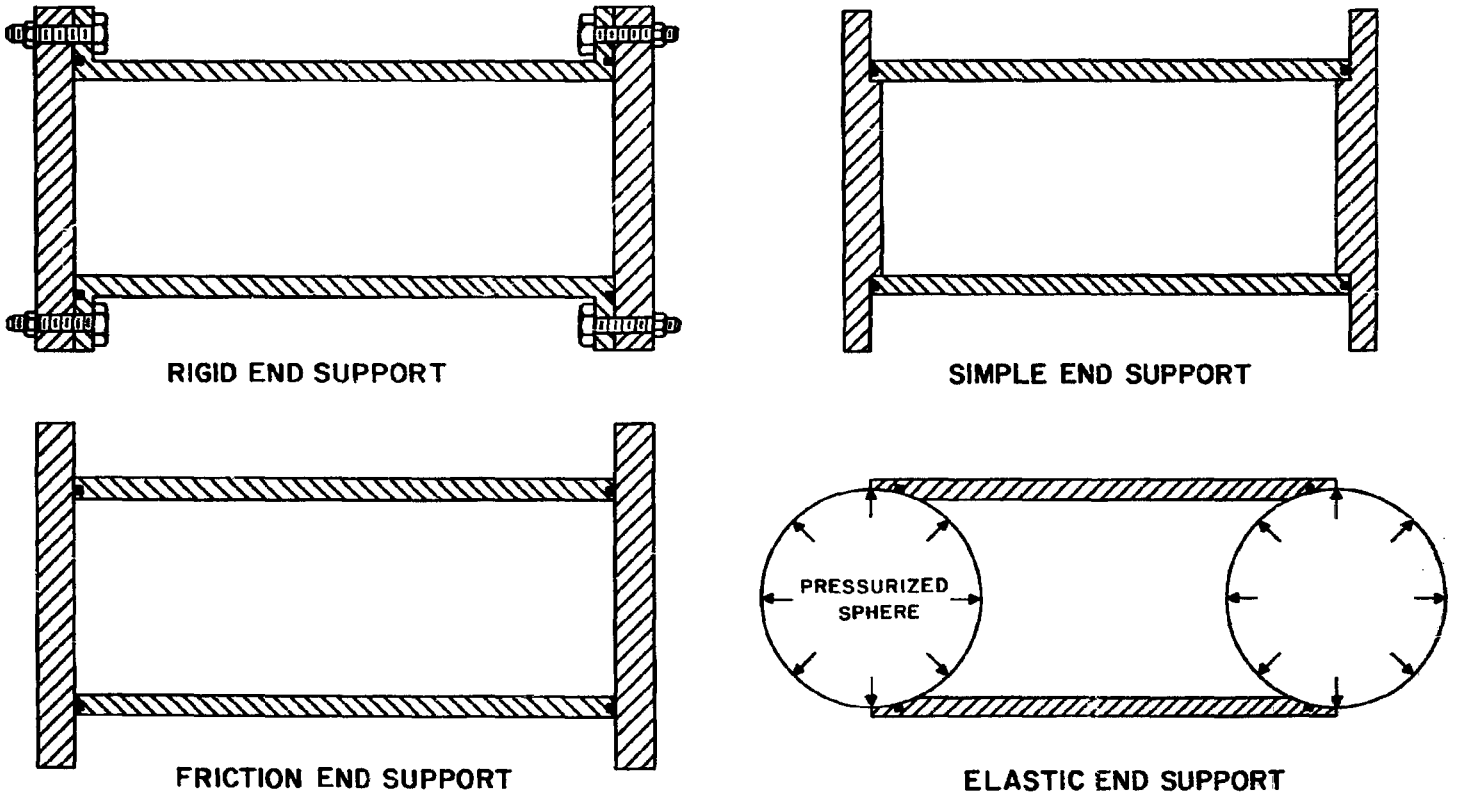

Fig. 13 - End Supports for Shells Subjected to External Pressure

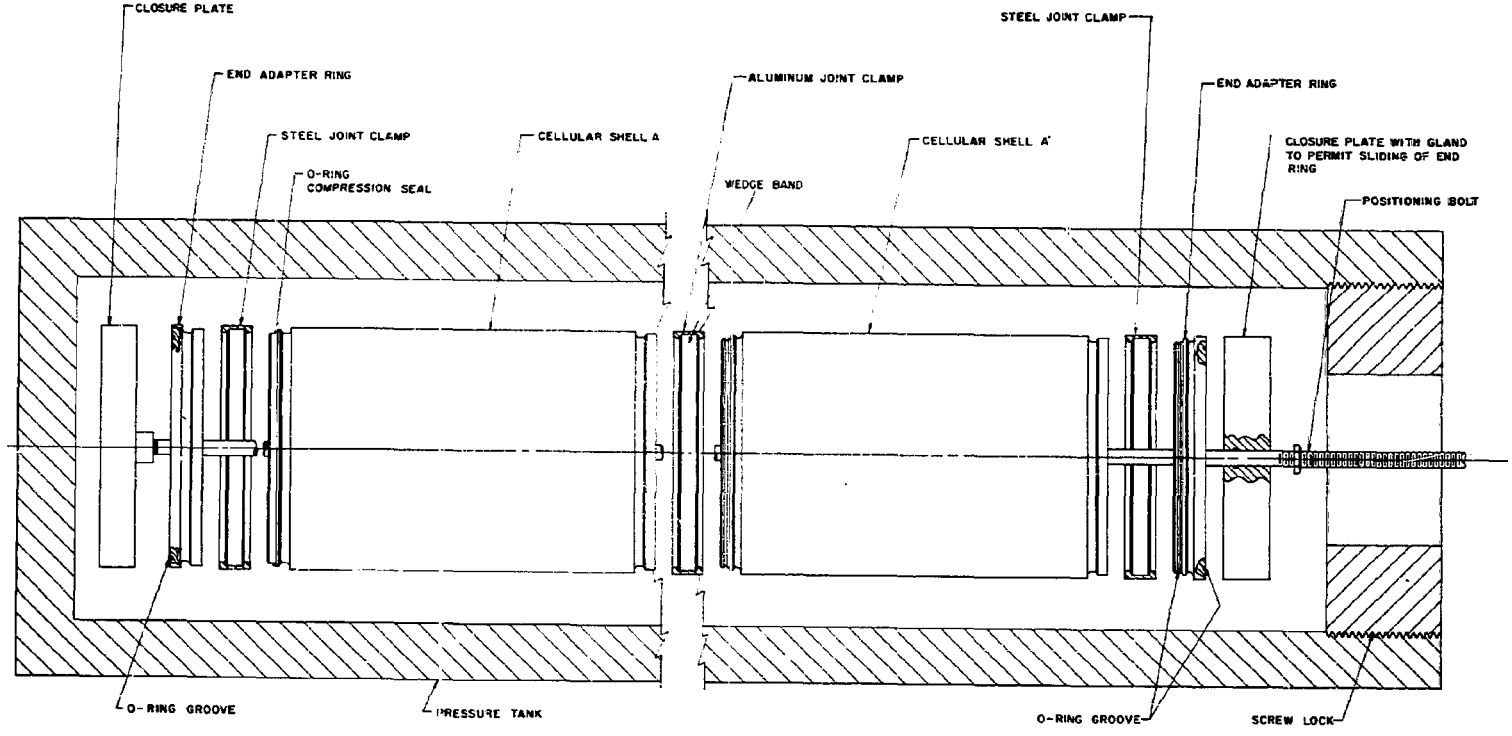

Fig. 14 - Method of Implosion Testing of Aluminum Cellular Sandwich Shells

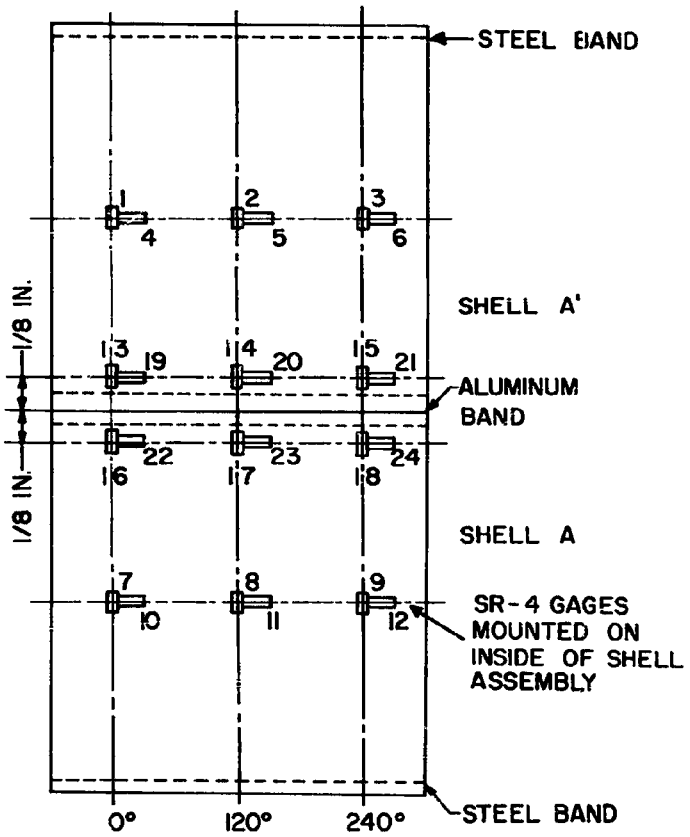

Fig. 15 - Location of Instruments during Pressure-Cycling Test

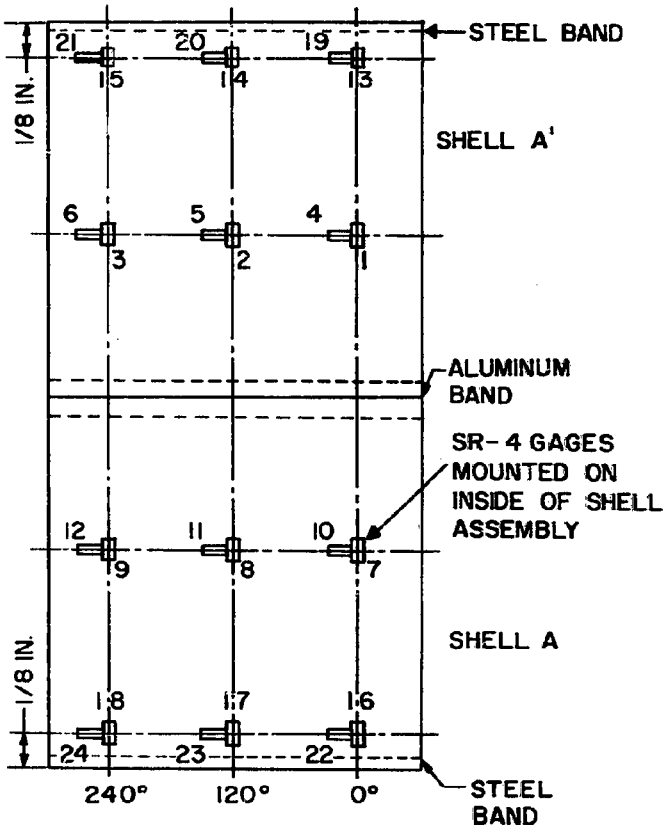

Fig. 16 - Location of Instruments during Implosion Test

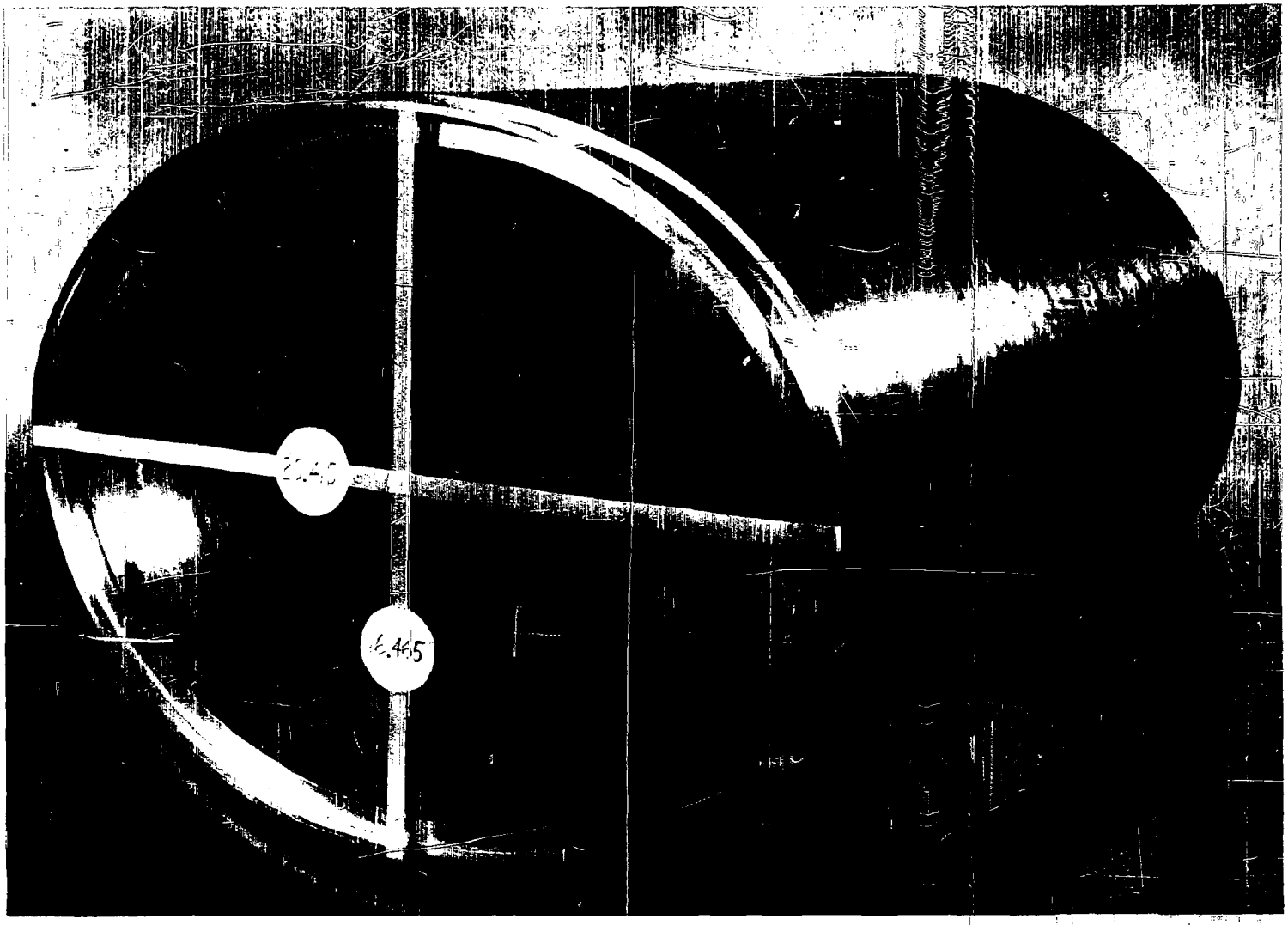

Fig. 17 - Cellular Sandwich Shell after Implosion

X (in.)	O.D. MIN. (in.)	O.D MAX. (in.)
0	18.44	22.90
5	18.21	22.79
10	18.23	22.80
15	18.23	22.78
20	18.40	22.51
25	18.50	22.47
29.25	19.01	22.32
0	19.41	22.34
5	19.41	21.85
10	19.82	21.60
15	19.92	21.35
20	20.22	21.10
25	20.40	21.00
29.25	20.51	20.90

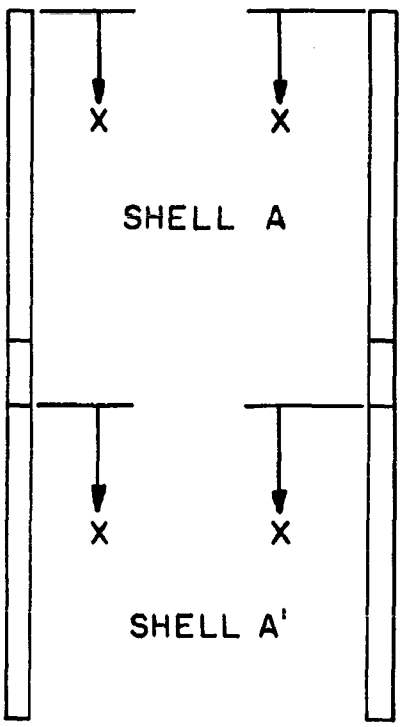

Fig. 18 - Deformation of Cellular Sandwich Shells after Implosion

Fig. 19 - Dissected Collapsed Shell (Model A)

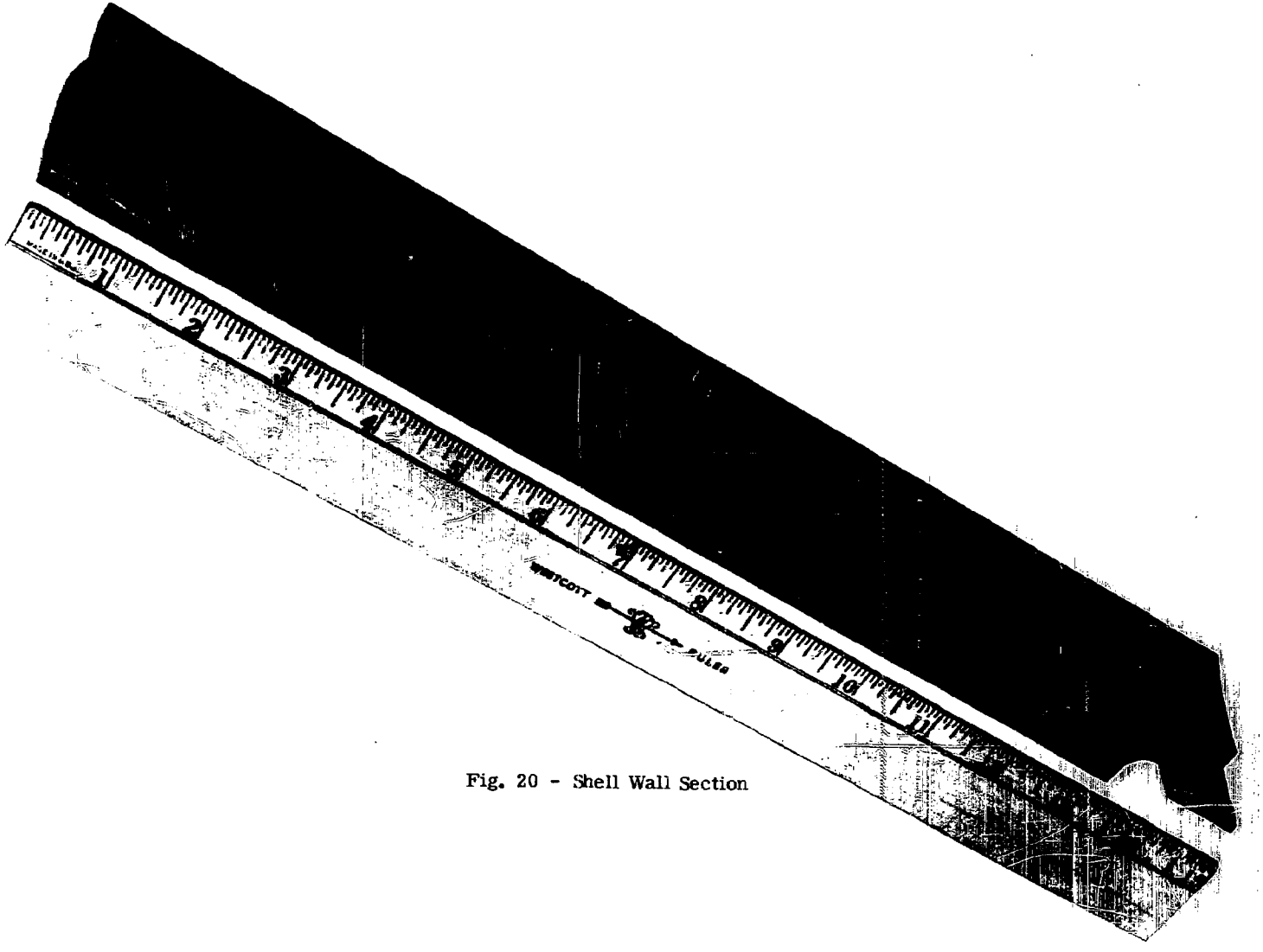

Fig. 20 - Shell Wall Section

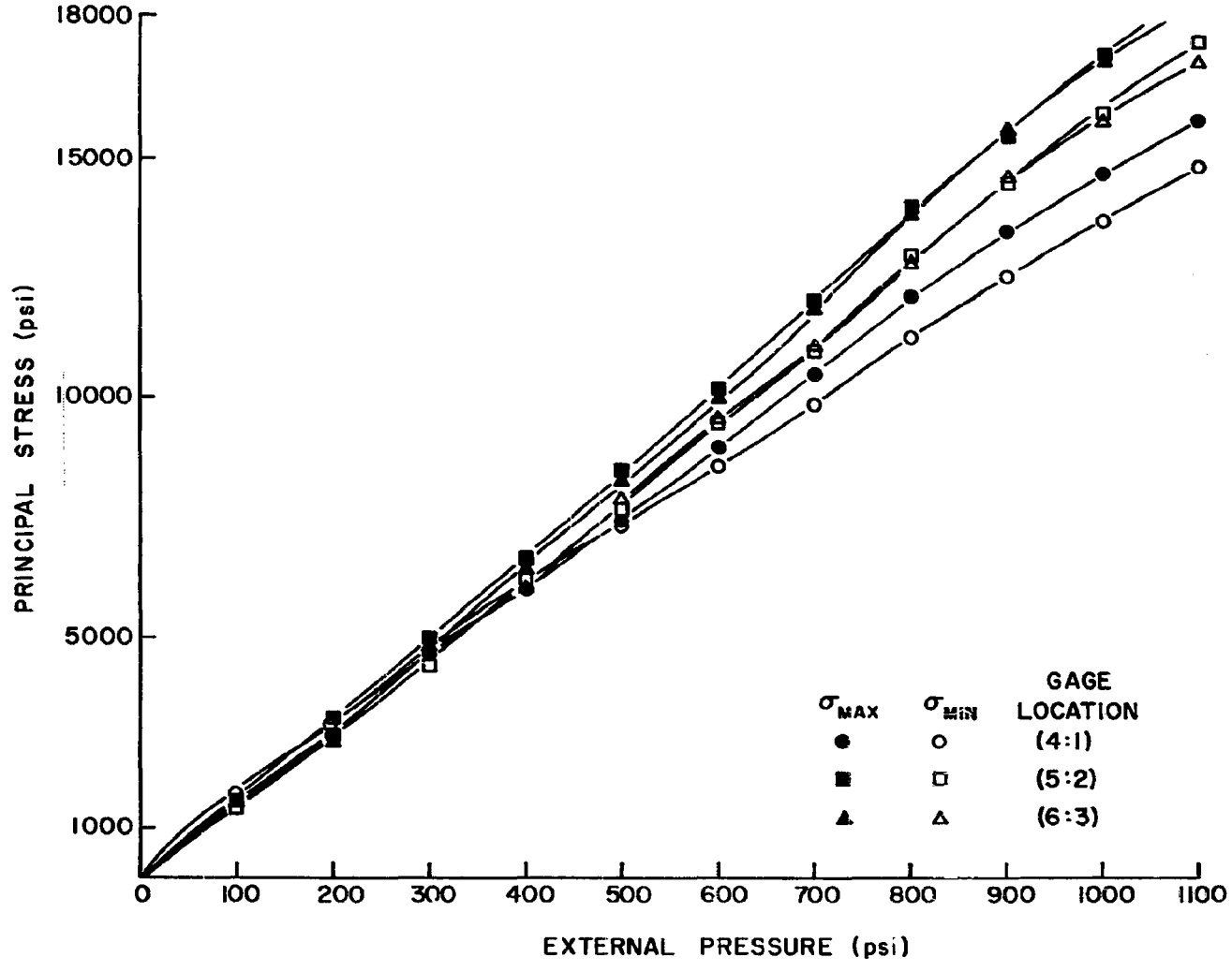

Fig. 21 - Stresses in Shell Models A and A' during Pressure Cycling - Locations 1 through 6 (See Fig. 15)

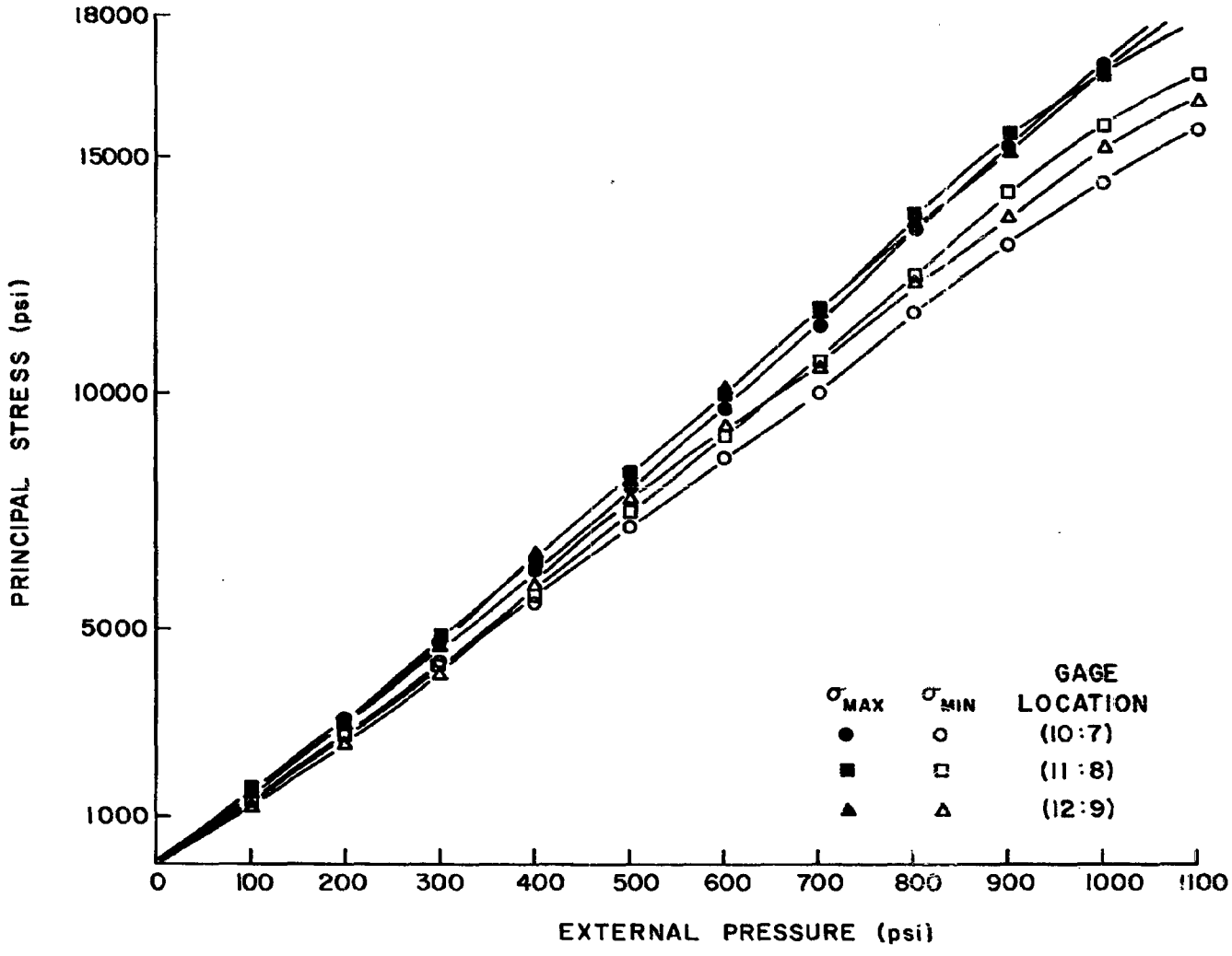

Fig. 22 - Stresses in Shell Models A and A' during Pressure Cycling - Locations 7 through 12 (See Fig. 15)

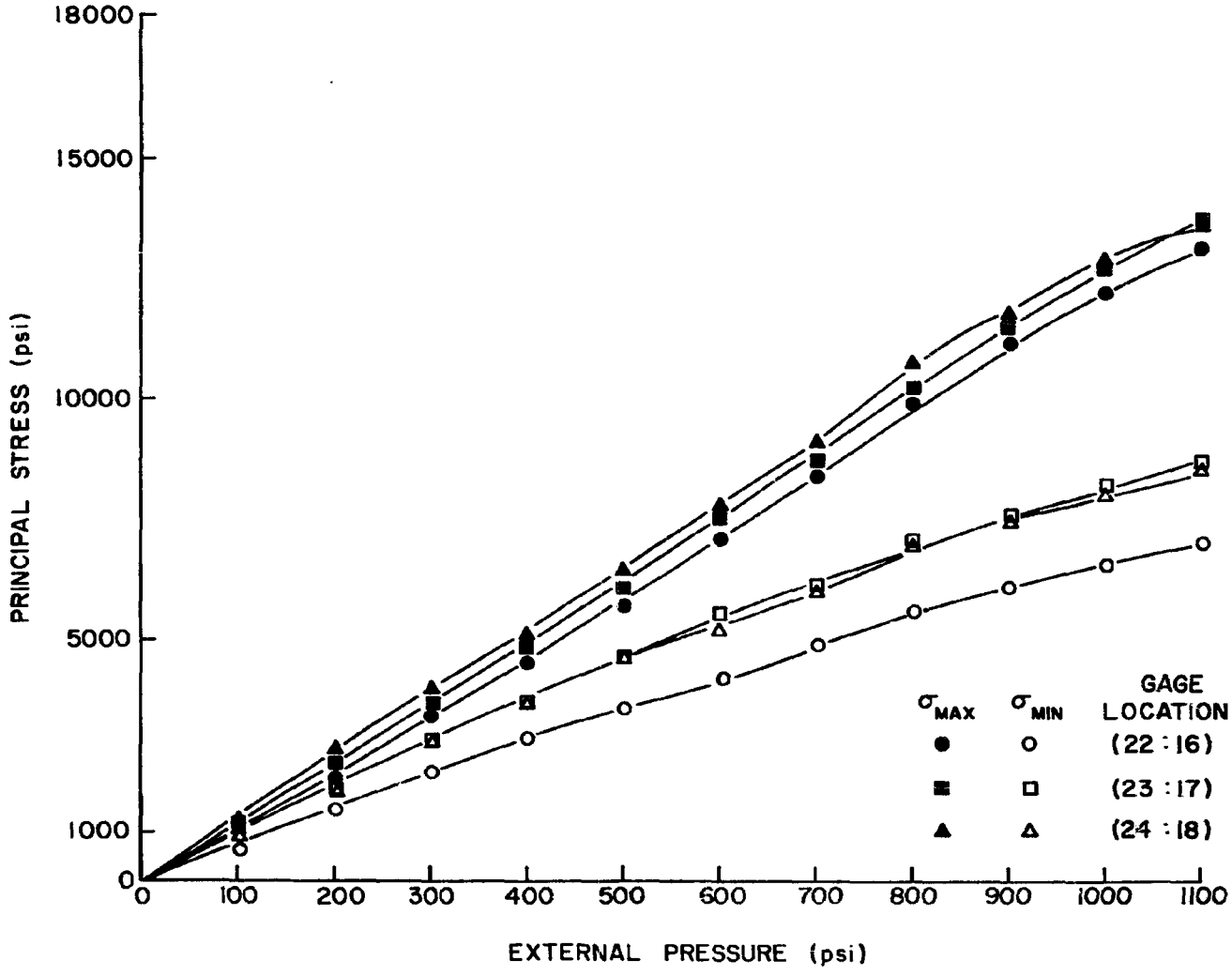

Fig. 23 - Stresses in Shell Models A and A' during Pressure Cycling - Locations 16 through 18 and 22 through 24 (See Fig. 15)

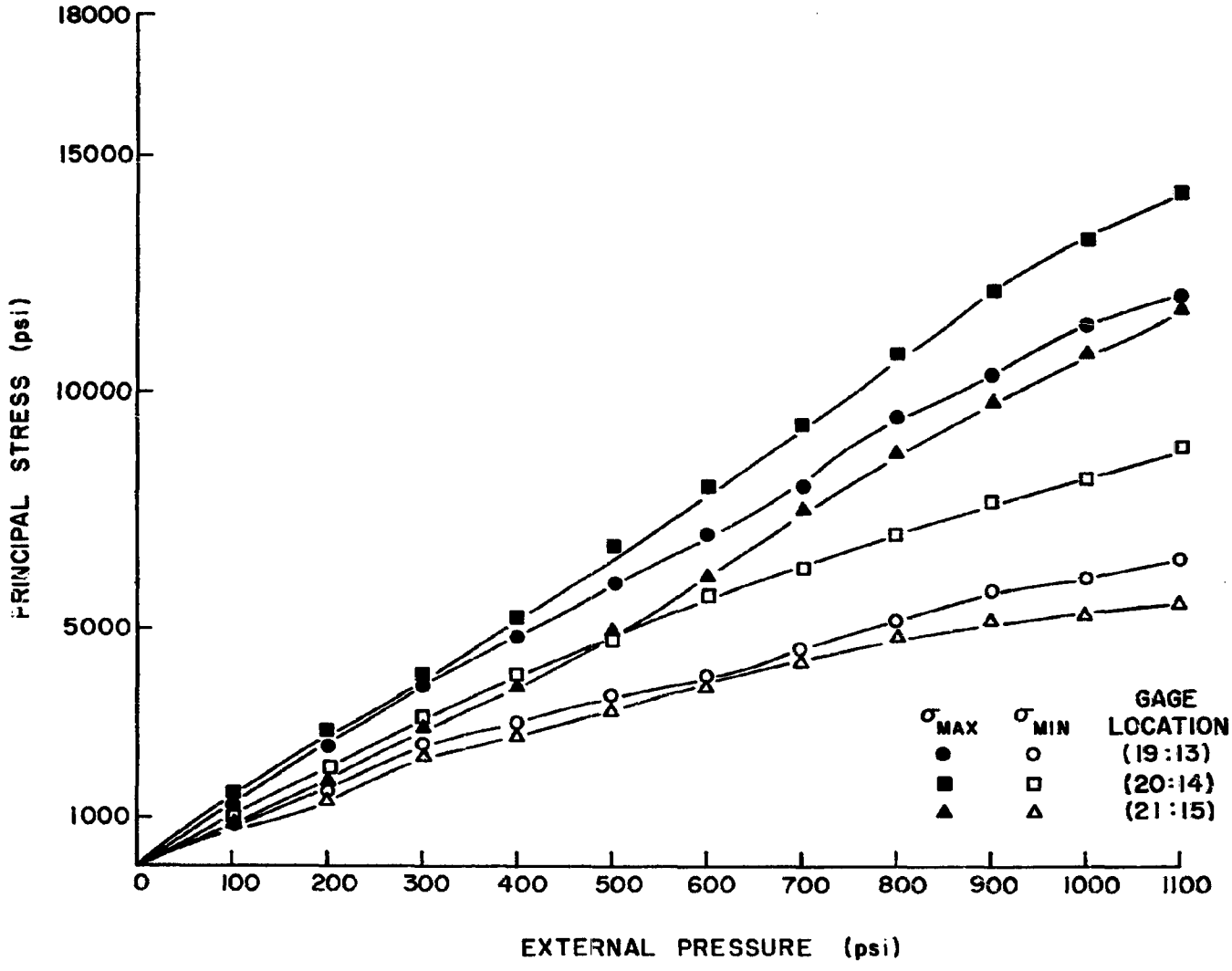

Fig. 24 - Stresses in Shell Models A and A' during Pressure Cycling - Locations 13 through 15 and 19 through 21 (See Fig. 15)

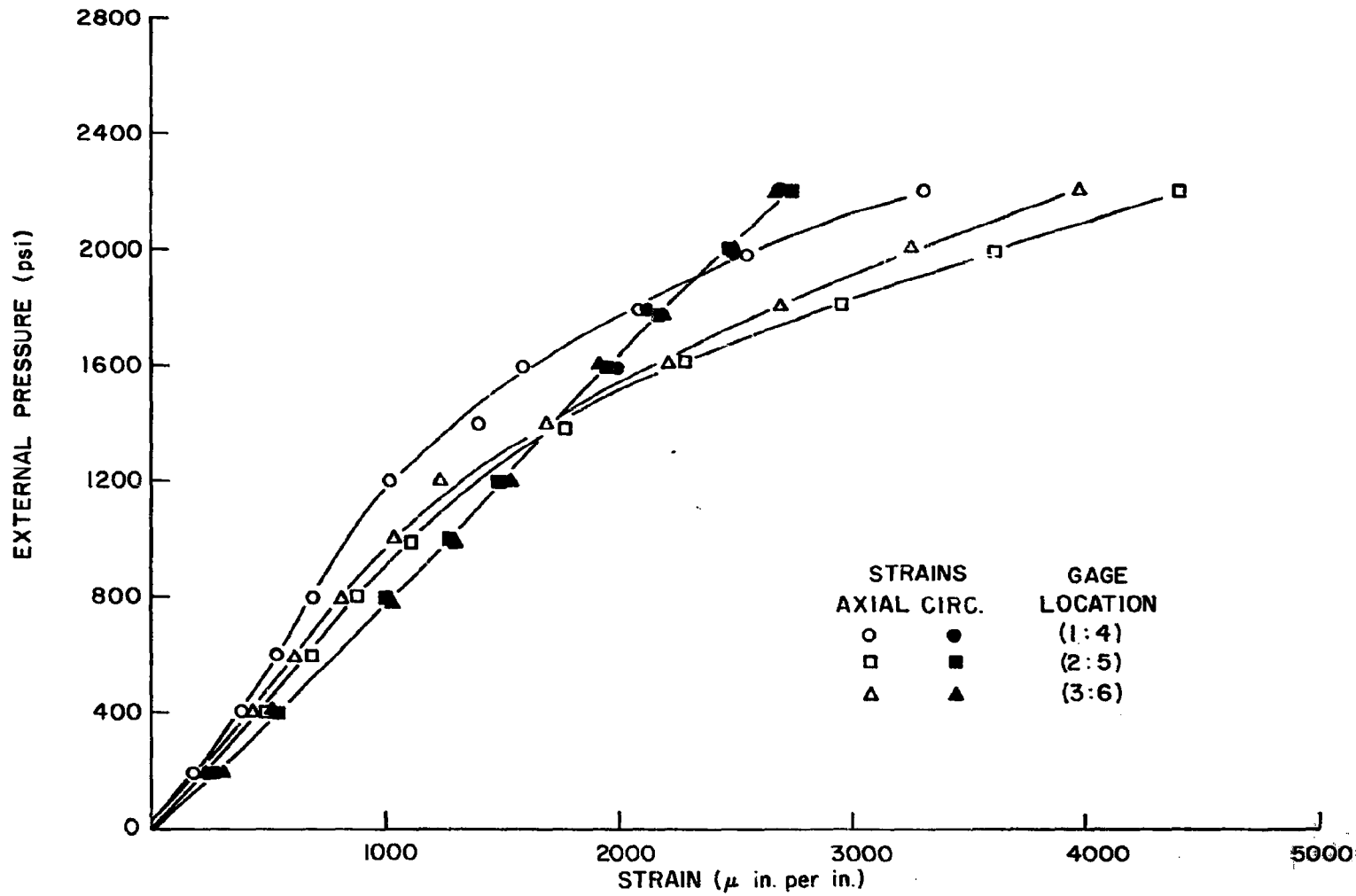

Fig. 25 - Strains in Shell Models A and A' during Implosion Testing - Locations 1 through 6 (See Fig. 16)

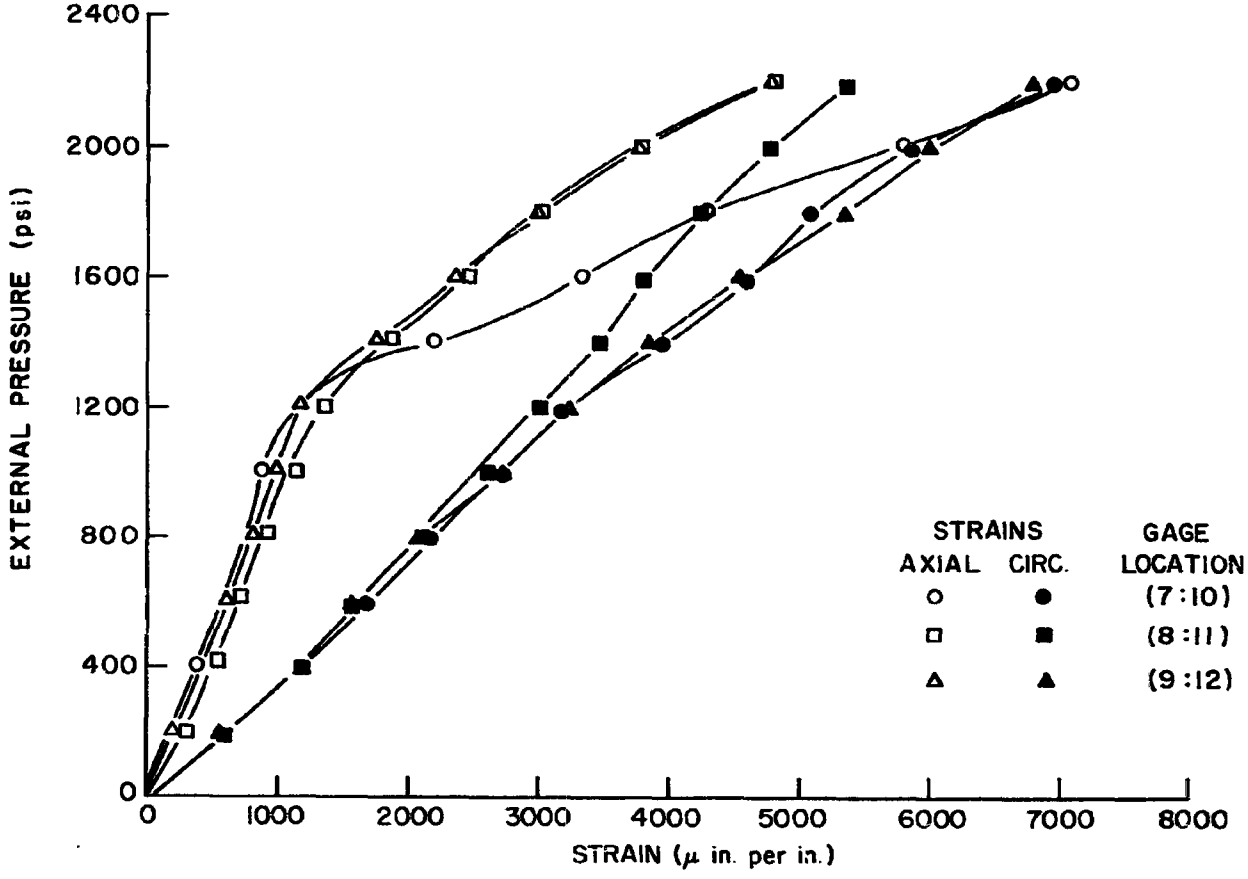

Fig. 26 - Strains in Shell Models A and A' during Implosion Testing - Locations 7 through 12 (See Fig. 16)

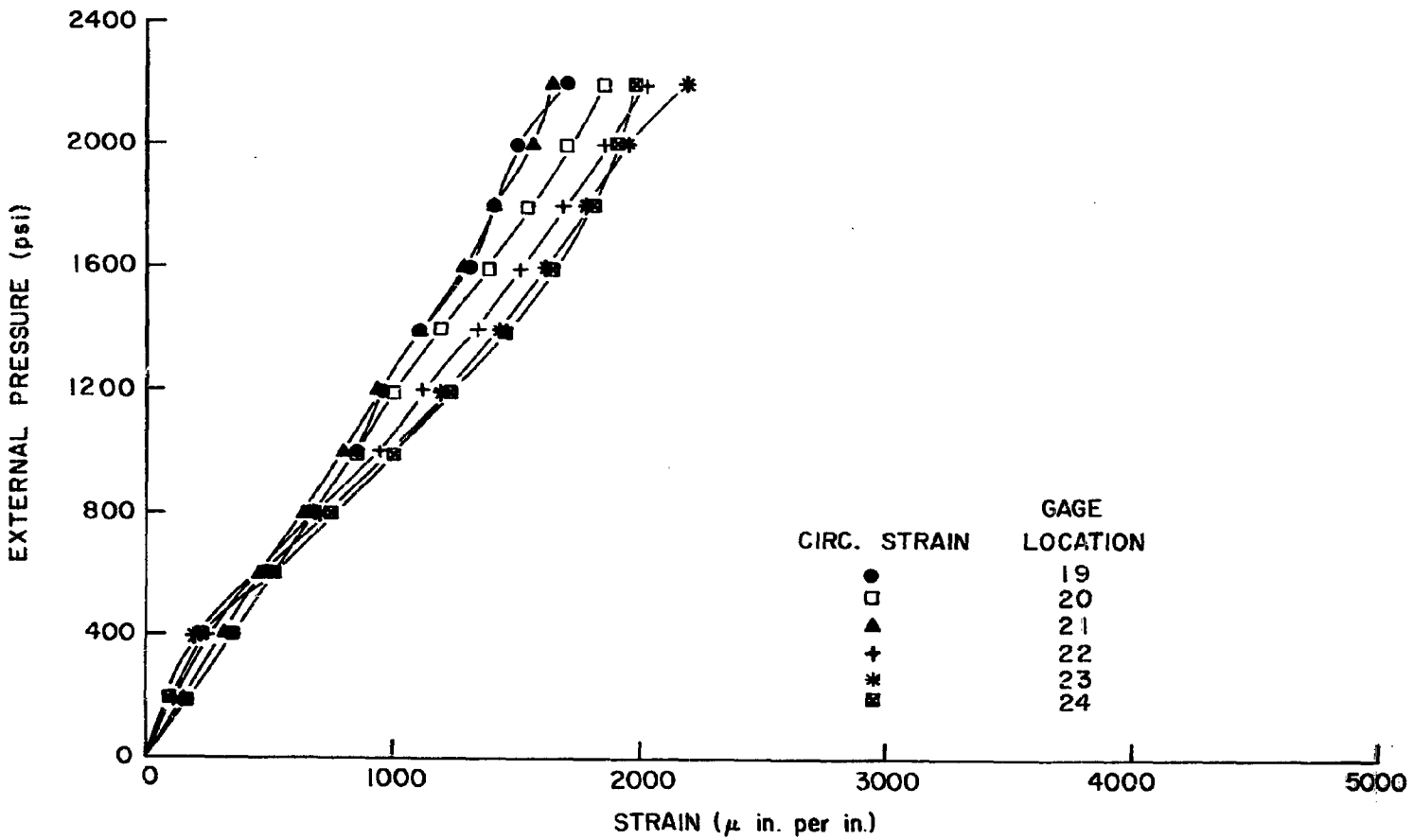

Fig. 27 - Strains in Shell Models A and A' during Implosion Testing - Locations 19 through 24 (See Fig. 16)

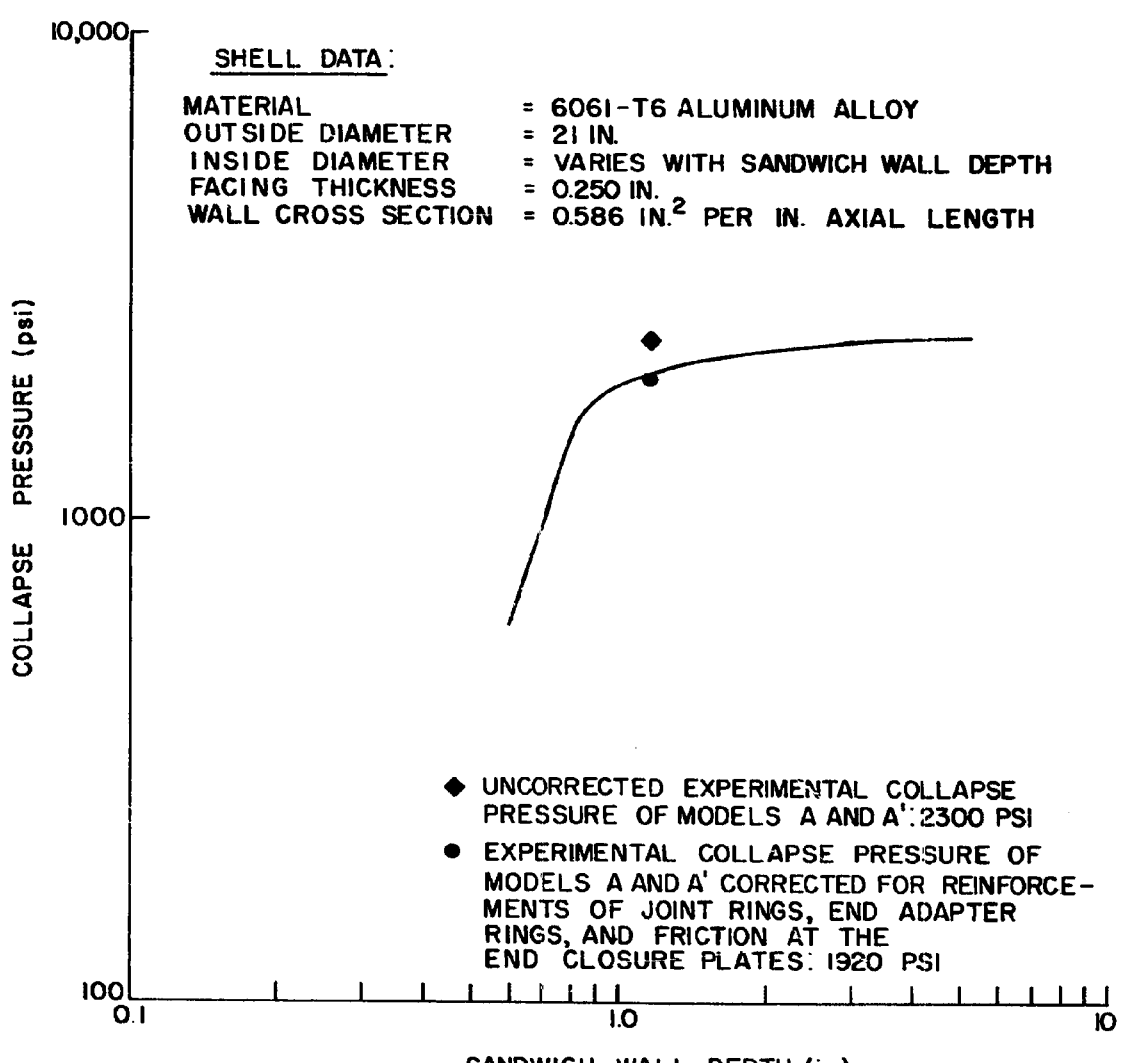

Fig. 28 - Collapse Pressure of an Infinitely Long Aluminum Cellular Sandwich Shell

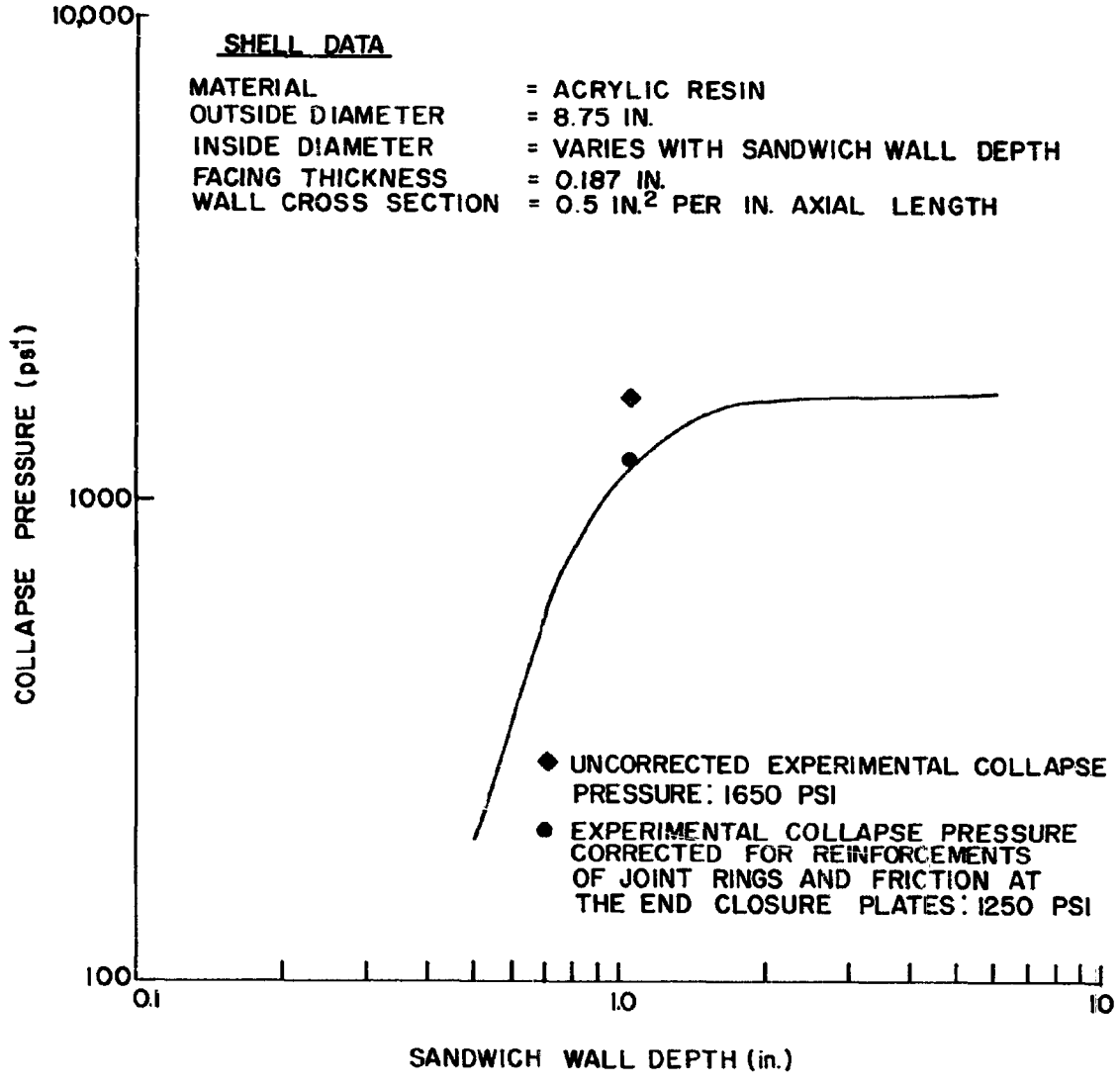

Fig. 29 - Collapse Pressure of an Infinitely Long Acrylic Resin Cellular Sandwich Shell

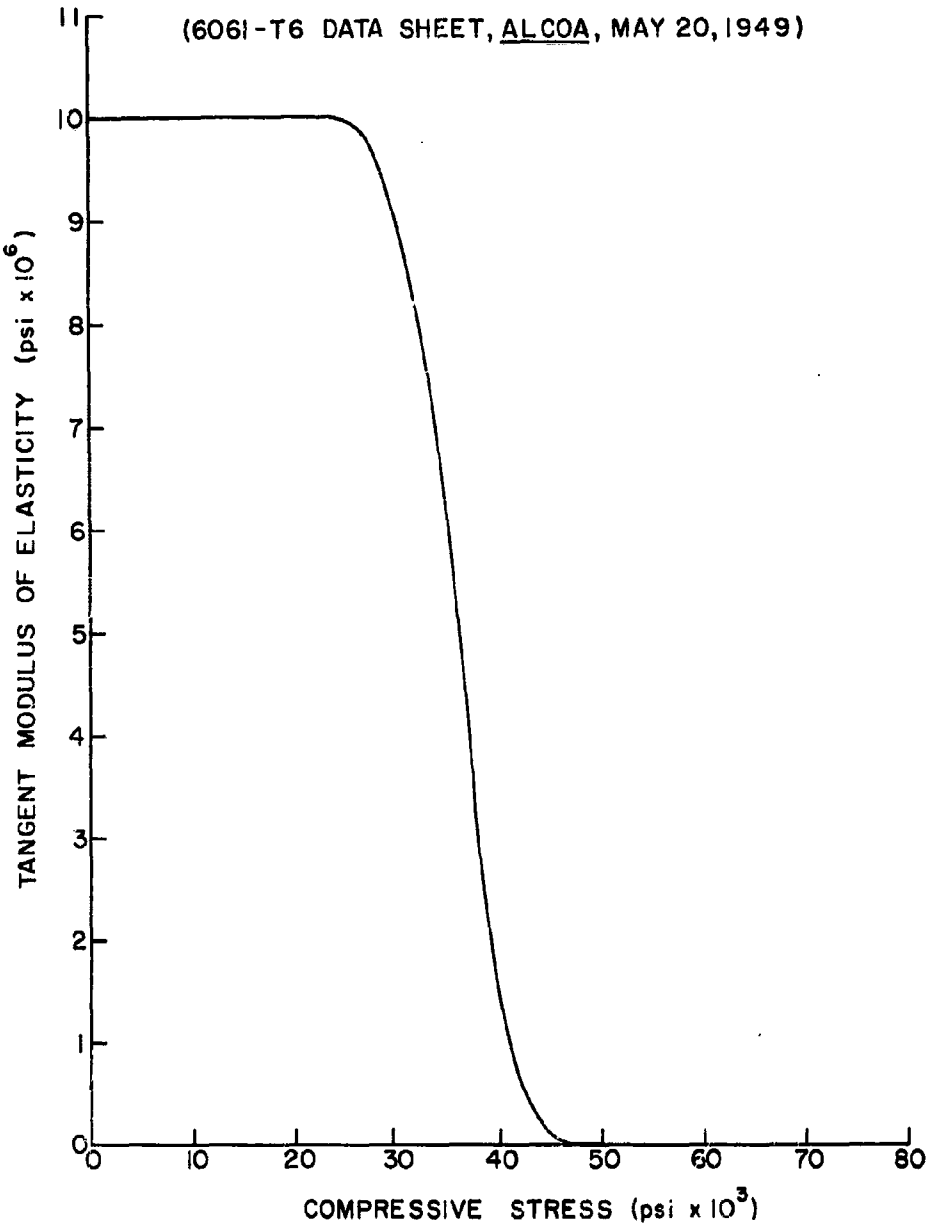

Fig. 30 - Tangent Modulus of Elasticity vs Compressive Stress for 6061-T6 Aluminum Alloy

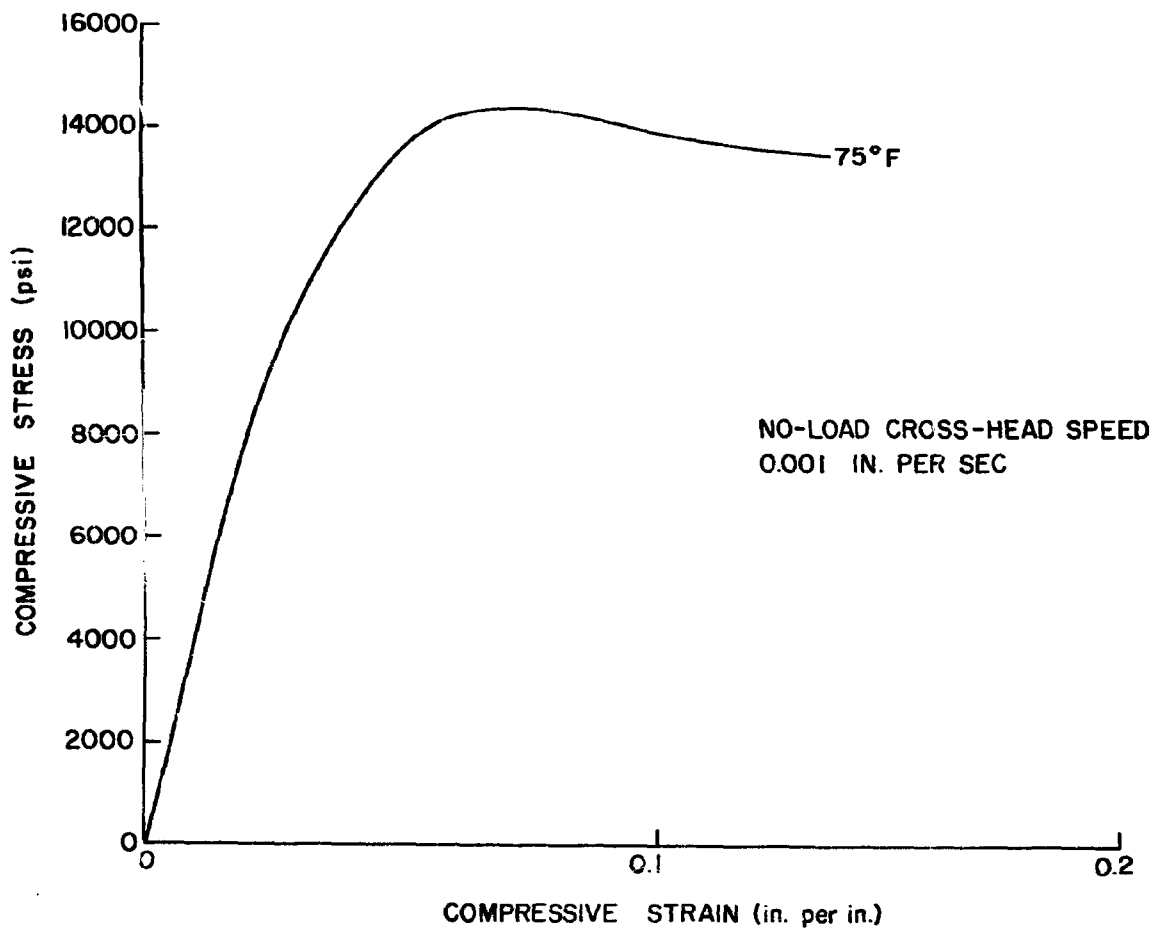

Fig. 31 - Stress-Strain Curve for Acrylic Resin Shell Material

UNCLASSIFIED

Ordnance Research Laboratory Report No. NOrd 16597-91
The Pennsylvania State University, University Park, Pa.

GENERAL INSTABILITY OF CIRCUMFERENTIALLY STIFFENED SANDWICH SHELLS SUBJECTED TO UNIFORM EXTERNAL PRESSURE

J. D. Stachiw

December 10, 1962; 13 pp. & figs.

The Bresse equation for the buckling of rings under radial pressure is modified to predict the general-instability collapse pressure of cellular sandwich shells under hydrostatic pressure. The validity of the equation is demonstrated by implosion experiments with carefully designed cellular sandwich shells, the general-instability collapse pressures of which are compared with the results obtained by the modified Bresse equation. The results indicate that the modified equation predicts the general-instability collapse pressure of cellular sandwich shells within 5 per cent. This equation is recommended for use only when the ratio of shell ring depth to shell mean diameter is less than 0.1.

UNCLASSIFIED

UNCLASSIFIED

Ordnance Research Laboratory Report No. NOrd 16597-91
The Pennsylvania State University, University Park, Pa.

GENERAL INSTABILITY OF CIRCUMFERENTIALLY STIFFENED SANDWICH SHELLS SUBJECTED TO UNIFORM EXTERNAL PRESSURE

J. D. Stachiw

December 10, 1962; 13 pp. & figs.

The Bresse equation for the buckling of rings under radial pressure is modified to predict the general-instability collapse pressure of cellular sandwich shells under hydrostatic pressure. The validity of the equation is demonstrated by implosion experiments with carefully designed cellular sandwich shells, the general-instability collapse pressures of which are compared with the results obtained by the modified Bresse equation. The results indicate that the modified equation predicts the general-instability collapse pressure of cellular sandwich shells within 5 per cent. This equation is recommended for use only when the ratio of shell ring depth to shell mean diameter is less than 0.1.

UNCLASSIFIED

UNCLASSIFIED

Ordnance Research Laboratory Report No. NOrd 16597-91
The Pennsylvania State University, University Park, Pa.

GENERAL INSTABILITY OF CIRCUMFERENTIALLY STIFFENED SANDWICH SHELLS SUBJECTED TO UNIFORM EXTERNAL PRESSURE

J. D. Stachiw

December 10, 1962; 13 pp. & figs.

The Bresse equation for the buckling of rings under radial pressure is modified to predict the general-instability collapse pressure of cellular sandwich shells under hydrostatic pressure. The validity of the equation is demonstrated by implosion experiments with carefully designed cellular sandwich shells, the general-instability collapse pressures of which are compared with the results obtained by the modified Bresse equation. The results indicate that the modified equation predicts the general-instability collapse pressure of cellular sandwich shells within 5 per cent. This equation is recommended for use only when the ratio of shell ring depth to shell mean diameter is less than 0.1.

UNCLASSIFIED

UNCLASSIFIED

Ordnance Research Laboratory Report No. NOrd 16597-91
The Pennsylvania State University, University Park, Pa.

GENERAL INSTABILITY OF CIRCUMFERENTIALLY STIFFENED SANDWICH SHELLS SUBJECTED TO UNIFORM EXTERNAL PRESSURE

J. D. Stachiw

December 10, 1962; 13 pp. & figs.

The Bresse equation for the buckling of rings under radial pressure is modified to predict the general-instability collapse pressure of cellular sandwich shells under hydrostatic pressure. The validity of the equation is demonstrated by implosion experiments with carefully designed cellular sandwich shells, the general-instability collapse pressures of which are compared with the results obtained by the modified Bresse equation. The results indicate that the modified equation predicts the general-instability collapse pressure of cellular sandwich shells within 5 per cent. This equation is recommended for use only when the ratio of shell ring depth to shell mean diameter is less than 0.1.

UNCLASSIFIED